Deliverable D30 (D4.9)

Summary: OP of PM, PM components and PM source contributions

RI-URBANS

Research Infrastructures Services Reinforcing Air Quality Monitoring Capacities in European Urban & Industrial AreaS (GA n. 101036245)

By

PSI, CSIC, NOA, CNRS & INERIS

17/01/2024

RI-URBANS (www.RIURBANS.eu) is supported by the European Commission under the Horizon 2020 – Research and Innovation Framework Programme, H2020-GD-2020, Grant Agreement number: 101036245

Deliverable D30 (D4.9): Summary: OP of PM, PM components and PM source contributions

Authors: Kaspar Rudolf Daellenbach (PSI), Andrés Alastuey (CSIC), Nikos Mihalopoulos (NOA), Gaëlle Uzu (CNRS), Xavier Querol (CSIC), Barend L. van Drooge (CSIC), Marjan Savadkoohi (CSIC), Meritxell Garcia-Marlès (CSIC), Olivier Favez (INERIS), Jean-Luc Jaffrezo & Vy Ngoc Thuy Dinh (CNRS)

Work package (WP)	WP4 Pilot implementations for testing and demonstrating services
Deliverable	D30 (D4.9)
Lead beneficiary	PSI
Deliverable type	■ R (document, report) ☐ DEC (websites, patent filings, videos,….) ☐ Other: ORDP (open research data pilot)
Dissemination level	■ PU (public) ☐ CO (confidential, only members of consortium and European Commission))
Estimated delivery deadline	M40 (31/1/2025)
Actual delivery deadline	17/01/2025
Version	Final
Reviewed by	WP4 leaders
Accepted by	Project coordination team
Comments	This report offers a summary of the analysis of novel air quality (AQ) metrics and source contributions at selected urban background locations in Europe. This includes emerging AQ metrics such as off-line particulate matter (PM) chemistry, equivalent Black Carbon (eBC), Particle Number Size Distribution (PNSD), as well as PM's oxidative potential (OP). Based on the presented work, main conclusions on source contributions in urban environments in Europe are drawn. The underlying data is available to the RI-URBANS partners at https://www.healthpilot-riurbans.eu.

RI-URBANS (www.RIURBANS.eu) is supported by the European Commission under the Horizon 2020 – Research and Innovation Framework Programme, H2020-GD-2020, Grant Agreement number: 101036245

Table of Contents

RI-URBANS (www.RIURBANS.eu) is supported by the European Commission under the Horizon 2020 – Research and Innovation Framework Programme, H2020-GD-2020, Grant Agreement number: 101036245

1 About this document

This report offers a summary of the analysis of novel air quality (AQ) metrics and source contributions at selected urban background locations in Europe. This includes emerging AQ metrics such as off-line particulate matter (PM) chemistry, equivalent Black Carbon (eBC), Particle Number Size Distribution (PNSD), as well as PM's oxidative potential (OP). Based on the presented work, main conclusions on source contributions in urban environments in Europe are drawn. The underlying data is available to the RI-URBANS partners at https://www.healthpilot-riurbans.eu.

This is a public document that will be distributed to all RI-URBANS partners for their use and submitted to the European Commission as a RI-URBANS Deliverable D30 (D4.9). This document can be downloaded at https://riurbans.eu/work-package-4/#deliverables-wp4.

2 Methods

In RI-URBANS, pilot cities were selected based such that 1) geographical variation in Europe is covered, and 2) large populations facilitate the potential use of the generated data in epidemiological assessments. Initially, Athens (Greece), Barcelona (Spain), and Zurich (Switzerland) were selected. Later on, Paris (France) - as one of the major metropolitan areas - was incorporated (see 2.1) even though not part of this deliverable. Measurement of novel metrics, including eBC, PNSD, PM composition and OP were performed following the recommendations of D1 (D1.1) generated within the framework of RI-URBANS WP1 and providing guidelines to measure the selected non-regulated pollutants and perform quality analysis.

2.1 Sampling sites

Within this deliverable, scientific work was carried out at four geographical locations (Figure 1): Athens Thissio (Greece), Barcelona Palau Reial (Spain), Paris Les Halles (France), and Zurich Kaserne (Switzerland).

Athens Thissio

The Athens Thissio Air Monitoring Station is located on the top of the hill of Nymphs at the National Observatory of Athens (37.97°N, 23.72° E) around 50 m above the mean city level. It is an urban background station close to the city centre, which receives aerosols both from urban and regional sources. Surrounding the area there is a pedestrian zone, while there is no major road within a 500 m radius from the station.

Barcelona Palau Reial

The Barcelona Palau Reial urban background monitoring site is located within the grounds of the IDAEA - CSIC in northwest Barcelona, *(41° 23'14.28"N, 2°6'56.34"E, 77* m a.s.l*),* located 200 m from one of the main traffic avenues of the city (Diagonal Avenue, traffic density of 90 000 vehicles per working day). The main source of atmospheric PM is road traffic, although contributions from industry, regional secondary atmospheric pollutants, construction, and shipping are also relevant. Atmospheric dynamics are driven by the breeze circulation regime, with a NW wind component during the night and the development of breezes during the day turning progressively from SE to SW direction, with gradually increasing wind speeds reaching maximum values around noon. This supersite is a National Facility (NF) for in situ measurements in ACTRIS - ERIC, and forms part of the Catalan Air Quality Monitoring Network (AQMN). It is a well-equipped infrastructure for in-situ characterization of aerosols (optical, physical, and chemical offline and online) and trace gases (NO_x, SO_2, O_3, CO).

RI-URBANS (www.RIURBANS.eu) is supported by the European Commission under the Horizon 2020 – Research and Innovation Framework Programme, H2020-GD-2020, Grant Agreement number: 101036245

Paris Les Halles

The urban background station at Paris-Les Halles is located in the city centre of Paris. It is fully operated by the AIRPARIF regional air quality monitoring network. The station is located in a public park (Jardins des Halles) adjacent to the infrastructure of the underground local public transportation network Châtelet Les Halles (48° 51' 43.74" N, 2° 20' 40.71"*W*). The surrounding area is a typical urban neighbourhood with residential and commercial activities. Boulevards and traffic roads are a few hundred meters from the site.

Zurich Kaserne

The Zurich Kaserne urban background monitoring site is located in a courtyard park in the city centre of Zurich (47° 22′ 42′′ N, 8° 31 ′52′′ E, 410 m a.s.l.), part of the Swiss National Monitoring Network (NABEL). The surrounding area is dominated by residential buildings and small businesses. While the station is not directly affected by major roads, local traffic is present. The station receives aerosols both from regional and local/urban sources.

***Figure 1**. Pilot 4 Monitoring sites: clockwise Athens, Barcelona, Paris and Zurich.*

RI-URBANS (www.RIURBANS.eu) is supported by the European Commission under the Horizon 2020 – Research and Innovation Framework Programme, H2020-GD-2020, Grant Agreement number: 101036245

2.2 Online measurement of novel metrics

2.2.1 Measurement of equivalent black carbon (eBC)

At all sites, eBC concentrations are measured and calculated by filter absorption photometers (FAPs) from Aethalometers (AE33) software through two steps here. In the first step (Step 1) the measured attenuation (ATN) is converted into absorption coefficient (ABS). For this, two artifacts related to the presence of the filter tape are considered. One artifact consists in an increase of the measured ATN due to the scattering of light by the filter tape (C_0). The other artifact consists in the progressive loss of sensitivity due to the progressive accumulation of particles on the filter tape (factor loading effect; FL). In the second step (Step 2) the ABS is converted into eBC mass concentrations assuming a specific and constant mass absorption cross section (MAC) of BC particles.

Step 1: All AE instruments convert ATN to ABS using predefined and constant C_0 that depends on the filter tape used. For the recent filter tape (M8060) C_0 is 1.39. The filter tape M8060 is the recommended one (available since October 2017). The C_0 values are set in the instrument software and must be changed manually if the filter tape is replaced with a different one (Savadkoohi et al., 2023). The AE33 model corrects online for FL by applying the "dual spot" method (Drinovec et al., 2015).

Step 2: The AE33 model calculates eBC from ATN at 880 nm using a MAC of 7.77 m^2g^{-1} at 880 nm and C_0=1.39 if the recommended filter tape is used.

Then eBC source apportionment is commonly performed using the Aethalometer (AE) approach (Sandradewi et al., 2008). This approach uses the seven wavelengths absorption coefficient measurements provided by AE instruments. ACTRIS provides the harmonization factors necessary to convert the ATN measured with AE instruments into ABS. These harmonization factors are needed because the C_0 is different from the one used in the AE software (see Savadkoohi et al., 2023, 2024, and ST2 on BC from RI-URBANS for more details).

2.2.2 Measurement of ultrafine particles (UFP)

Measurements of Particle Number Concentration (PNC) and Particle Number Size Distribution (PNSD) of UFP are conducted at all sites by using Condensation Particle Counters (CPCs) and Mobility particle size spectrometers (MPSSs), respectively, in accordance with ACTRIS and CEN guidelines and documents (ACTRIS, 2021; CEN/–S16976:2016; CEN/TS17434:2020), and ST1 on UFP-PNSD from RI-URBANS. These guidelines recommend a size measurement range of 10-800 nm and allow the measurement of particles with diameters below 10 nm if required. Data harmonisation is performed according to the methods described by (Trechera et al., 2023) and (Garcia-Marlès et al., 2024a). The data is averaged hourly, and the measurement range is limited to 10-800 nm to ensure better comparability between the sites.

2.3 PM composition and OP

2.3.1 Sampling and analytical strategies

Given the different chemical composition and sources of fine and coarse PM at each pilot city, PM2.5 and PM10 were sampled simultaneously for 1 year – 1 full seasonal cycle for subsequent chemical offline analyses. Due to constraints defined by the elaborate chemical characterization, not every day of the year was characterized but instead every 2nd day (Barcelona, Athens, Paris). Zurich was used as a frontrunner (sampled every 4th day) based on which the analytical strategy was defined, e.g. increased sampling frequency. This is more than for Zurich (every 4th) to allow for better data coverage, while keeping the analytical load under control.

To obtain large enough PM samples to perform all the analyses planned, PM sampling was performed by using high-volume samplers (HiVol, 30 m^3 h^{-1}; DH80 DIGITEL, Switzerland/Austria; and CAVA/MSb - MCV, Spain), equipped

RI-URBANS (www.RIURBANS.eu) is supported by the European Commission under the Horizon 2020 – Research and Innovation Framework Programme, H2020-GD-2020, Grant Agreement number: 101036245

with PM10 and PM2.5 inlets. The samples were collected on 15-cm diameter ultrapure quartz microfiber filters (Pall). Sampling period and number of samples collected at each site are shown in Table 1.

The PM mass on the filter was determined at some sites using the EN12341:2023 gravimetric procedures at each sampling location by the collecting institution. In short, gravimetric concentration of PM was obtained by weighing the filter samples before and after sampling, after 48 h stabilization at 20 °C and 50 % RH. For Paris, PMx measurements are achieved using automatic systems in agreement with EN16450:2017.

A very large and comprehensive chemical characterization was performed based on the PM2.5 and PM10 Quartz fiber filters (Pall). For optimal comparability of the results, each type of analysis was performed centrally in 1 lab, except for specific analysis in Paris that decided to join the activities later (and is not part of the deliverable). In these cases, an intercomparison with Pilot central labs was carried out. After gravimetric analysis, punches of filters were distributed to each laboratory for centralized analysis (Figure 2). Table 2 summarizes the analyses performed and the laboratory responsible for each analytical task.

Blank filters from the same filter box underwent the same sample treatment and measurements, and values were subtracted from the corresponding samples.

***Table 1**. Sampling period and number of samples collected and analysed at each site are shown.*

Site	Period	PM10 samples	PM2.5 samples
Zurich Kaserne	06/2018-05/2019	91	91
Barcelona Palau Reial	03/2022-02/2023	175	160
Athens Thissio	03/2022-02/2023	159	155
Paris Châtelet-Les Halles	04/2022-03/2023	124	169

RI-URBANS (www.RIURBANS.eu) is supported by the European Commission under the Horizon 2020 – Research and Innovation Framework Programme, H2020-GD-2020, Grant Agreement number: 101036245

***Table 2**. Laboratory and method for each PM component analysed.*

PM component	Responsible Laboratory	Method
Metals: **total concentration** **soluble fraction**	 CSIC NOA	 ICP-OES, ICP-MS ICP-MS
Water soluble ions	NOA Paris: CNRS	IC IC-MS (ions and organic acids)
OC/EC	CSIC Paris: INERIS(PM_{10}),AirParif ($PM_{2.5}$)	Thermo-optical analyser (SUNSET)
Brown carbon	NOA	UV–Vis spectrophotometry
Organic tracers: PAHs, Acids**,** Sugars and polyols	CSIC Paris: CNRS	GC-MS LC-MSMS. Includes tetrols
WSOC	PSI	Shimadzu TOC analyzer
Non-targeted mass spectral WSOA characterization	PSI	Aerosol Mass Spectrometer, extractive electrospray ionization MS
Brown Carbon (BrC) at all 4 sites	NOA	BrC in water- and methanol- extracts: UV–Vis spectrophotometry
Oxidative potential	CNRS	acellular OP^{AA} and OP^{DTT} assays

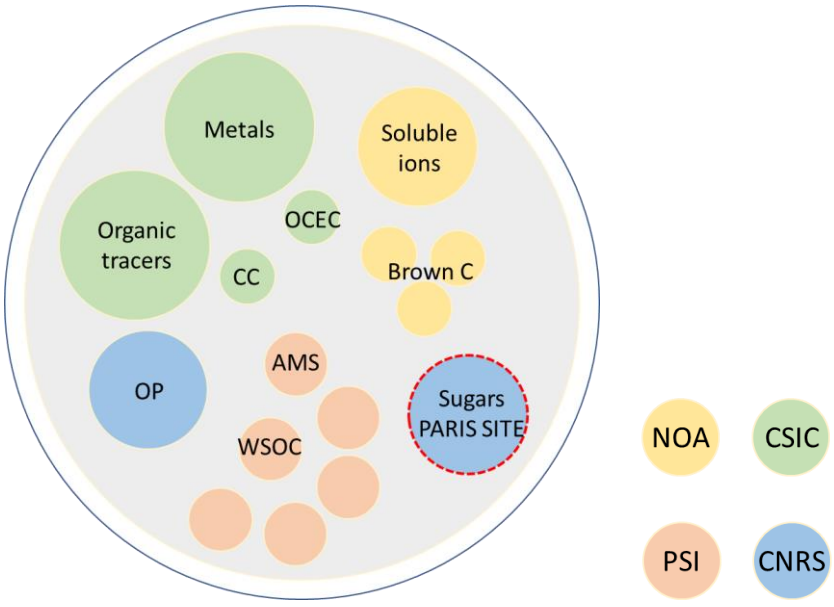

***Figure 2.** Distribution of punches for analysis.*

RI-URBANS (www.RIURBANS.eu) is supported by the European Commission under the Horizon 2020 – Research and Innovation Framework Programme, H2020-GD-2020, Grant Agreement number: 101036245

The offline chemical analyses performed at the pilot locations include the components put forward in the new EU AQ Directive EU 2024/2881/EC but go further in detail to explore the added value of specific source tracers. In the following, the protocols applied for performing the different chemical analyses are described in detail.

2.3.2 Total concentration of metals

Determination of concentration of major elements and metals was carried out at the IDAEA-CSIC laboratories following the methodology proposed by Querol et al. (2001). This method requires a complete previous dissolution of the samples (samples are bulk acidic dissolved using HNO_3:HF:$HClO_4$) and has been widely used. This procedure allows the complete digestion of silicon-containing compounds, and other specific minerals (e.g. TiO_2), which is required for source apportionment analyses where road dust, non-exhaust vehicle PM, demolition/construction dust or desert dust is intended to be included. Acidic digestion and analysis of all samples collected at all sites (including Zurich) was performed at the IDAEA-CSIC Laboratories.

One punch of 45 mm diameter of each sample underwent acid digestion pre-treatment (HNO_3:HF:$HClO_4$), and the resulting acidic solutions were subsequently analysed using Inductively Coupled Plasma Atomic Emission Spectrometry (ICP-AES, ICAP 6500 Radial View, Thermo Fisher Scientific, US) to determine the concentration of major elements (Al, Ca, Cu, Fe, K, Mg, Mn, Na, P, and S) and Inductively Coupled Plasma Mass Spectrometry (ICP-MS, iCAP-RQ, Thermo fisher Scientific, US) to measure the concentration of trace elements (Li, Be, Sc, Ti, V, Cr, Mn, Co, Ni, Cu, Zn, Ga, Ge, As, Se, Rb, Sr, Y, Zr, Nb, Mo, Cd, Sn, Sb, Cs, Ba, La, Ce, Pr, Nd, Sm, Eu, Gd, Tv, Dy, Ho, Er, Tm, Yb, Lu, Hf, Ta, W, Tl, Pb, Bi, Th, and U). The accuracy of the ICP-AES and ICP-MS analyses was investigated by analysing 3–10 mg of the National Institute for Standards and Technology-1633b (fly ash) reference material loaded on a 150-mm blank filter (Amato et al., 2009). See ST3 on PM speciation from RI-URBANS.

2.3.3 Water soluble ions

Analysis of water-soluble ions followed the standard (EN16913:2017). Water extraction was performed at NOA labs for samples collected at Athens and Barcelona. The same constituents for Paris and Zurich were analysed by CNRS. At first, a piece with 1.5 cm^2 surface area was obtained from each filter that collected atmospheric samples and from blanks, using appropriate tools. The pieces were then placed inside dry plastic bottles and extracted with 10mL of ultrapure water. Then, they were placed inside an ultrasound system for 45 minutes to aid dilution. After the extraction, the bottles were left to cool down and a few chloroform ($CHCl_3$) drops were added in order to prevent bacterial deterioration and preserve the concentrations while the samples were stored in the fridge until analysis. The major aerosol cations (Ca^{2+}, Mg^{2+}, Na^+, K^+, NH_4^+) and anions (SO_4^{2-}, NO_3^-, Cl^-) were analyzed by Ion Chromatography (IC; Dionex-500; Thermo Fisher Scientific) following the methodology described in (Paraskevopoulou et al., 2015). All analytical results were blank-corrected. For the anions the mobile phase used was a mixture of sodium bicarbonate and sodium carbonate $NaHCO_3$ / NaH_2CO_3 with an isocratic elution flow rate of 1.5 mL/min. For the cations (NH_4^+, Na^+, K^+, Mg^{2+}, Ca^{2+}) the mobile phase used is methanesulfonic acid (MSA), a strong acid that dissociates and releases H^+ which substitutes the cations inside the column. Isocratic elution with a flow rate of 1 mL/min was selected. Before analyzing the extracted samples, each sample was filtered using a CHROMAFIL 0.15 µm with 0.45 µm pore size filter and then transferred inside smaller glass vials that were placed on the autosampler. This way particles or impurities that could damage the chromatography system were removed. See ST3 on PM speciation from RI-URBANS.

2.3.4 Water soluble concentration of metals

The water extraction solution (2.3.3) was used for the analysis of water soluble metals by using an Inductively Coupled Plasma Mass Spectrometry (ICP-MS, Perkin Elmer, NexION 300X). Water soluble fractions of trace elements (Al, Ca, Mn, Fe, V, Cr, Ni, Cu, Zn, Cd, As and Pb) were determined by following the procedure described in

RI-URBANS (www.RIURBANS.eu) is supported by the European Commission under the Horizon 2020 – Research and Innovation Framework Programme, H2020-GD-2020, Grant Agreement number: 101036245

Theodosi et al. (2018). Yttrium (Y) and Indium (In) were added as internal standards, and all reported concentrations were corrected for blanks. This analysis was performed at NOA for Barcelona, Zurich, Paris and Athens samples.

2.3.5 Organic and elemental carbon

To determine the concentration of OC and EC collected in quartz fibre filters we follow the EN16909:2017 standard, for the measurement of airborne EC and OC in PM2.5 (Karanasiou et al., 2015; Brown et al., 2017). The European Committee for Standardisation (CEN) Technical Committee 264 'Air Quality' adopted the thermal-optical offline analysis with transmittance correction and the EUSAAR2 thermal protocol (Cavalli et al., 2010) as the reference methodology for the determination of EC and OC in ambient PM2.5 (EN16909:2017). All filters were analysed using thermal-optical analysis (Sunset analyzer), by Ineris (PM10) and AIRPARIF (PM2.5) for the Paris site and by IDAEA-CSIC for the other sites. These 3 laboratories regularly participate in the intercomparison exercises organised by the JRC (now as part of ACTRIS/CAIS-ECAC activities). See ST3 on PM speciation from RI-URBANS.

2.3.6 Brown carbon

Brown carbon (BrC) measurements in water- and methanol-extracts were performed by UV–Vis spectrophotometry (Hecobian et al., 2010; Srinivas et al., 2016). A 1 cm2 punch was placed in 15 mL of ultrapure water. The water-soluble fraction was extracted by ultrasonication for 30 min (Paraskevopoulou et al., 2023). The absorption of water-soluble fraction was determined at 365 and 590 nm, allowing for the calculation of Absorption Ångström Exponent (AAE) in the range of 365-590 nm, as described in detail by Paraskevopoulou et al., 2023.

2.3.7 Organic tracers

The analysis of molecular organic compounds involved solvent extraction followed by gas chromatography-mass spectrometry (GC-MS), enabling the detection and quantification of a wide range of organic compounds with varying polarities. Up to seventy-two compounds were detected in ambient air and emission sources, many of which serve as molecular tracers of sources and atmospheric processes (Alier et al., 2013). Modifications of the extraction method described by Fontal et al (2015) were implemented and described by Van Drooge et al. (2023)

A filter punch (3.4 mm diameter) was taken from whole filter samples and placed in a conical vial, and 25 µL of deuterated PAH standard (50 ppb) in cyclo-hexane was added for PAH analysis. Another punch sample was taken from the whole PM filter to be analysed for acids and sugars, and 25 µL methanol containing deuterated succinic acid-D4 and levoglucosan-D7 (3 ppm) was added to this vial. Extraction took place in an ultrasonic bath for 15 minutes. Then, the filter punches were removed from the vials, and the PAHs extracts were directly injected into GC-MS. The acid and sugar extracts were evaporated to dryness under gentle nitrogen gas stream and 25 µL bis(trimethylsilyl)trifluoroacetamide (BSFTA)+ 1% TMCS and 10 µL pyridine was added to vial to facilitate the formation of trimethylsilyl (TMS) derivatives of polar compounds for 30 minutes at 70ºC in oven before injection into GC-MS. Instrumental analysis was conducted using a GC-MS (Agilent 7890 GC with 5975 MSD), operating in full scan mode with electron impact ionization for polar compounds and in SIM mode for PAHs. Compound quantification utilized an internal standard method and corrections were made for procedural losses using surrogate standards. Field and analytical blanks were performed during sample analysis. Identified organics were confirmed by retention time, characteristic mass fragments, and comparison with spectral libraries. Organic compounds were analysed and identified based on their mass spectra and retention times. See ST3 on PM speciation from RI-URBANS.

RI-URBANS (www.RIURBANS.eu) is supported by the European Commission under the Horizon 2020 – Research and Innovation Framework Programme, H2020-GD-2020, Grant Agreement number: 101036245

2.3.8 Non-targeted chemical characterization of water-soluble OA

As explorative addition, the water-soluble organic PM fraction was characterized based on aqueous extractions of a filter portion in milliQ water, following the protocols presented in Daellenbach et al. (2016, 2020) and Cui et al. (2024). In a first step, the bulk quantities water-soluble organic carbon and water-soluble inorganic carbon were quantified with a Shimadzu TOC analyzer. In a next step, the same extracts were used for non-targeted chemical characterisation. For Zurich, such analyses were performed using an Aerosol Mass Spectrometer following the approaches presented in Cui et al (2024). The results showed a good chemical resolution while still limited by the hard ionization in the mass spectrometer leading to excessive fragmentation of the analyses. This resulted in a loss of chemical information. For that reason, we used a soft-ionization mass spectrometer (Extractive Electrospray Ionization Mass Spectrometer: EESI-MS) for Athens, Barcelona, and Paris following Cui et al. (2024).

2.3.9 Oxidative potential

PM's oxidative potential was measured with two complementary assays relying on Ascorbic Acid (AA) and dithiothreitol (DTT). The PM collected on quartz fibre filters was extracted in simulated lung fluid (no filtration step to keep the insoluble parts) at iso-concentrations of 25 µg/ml. The protocols followed Calas et al. (2017, 2018, 2019). See ST4 on OP of PM from RI-URBANS.

2.3.10 Mass closure / data treatment

PM components determined have been grouped into: organic matter (OM) derived from OC, elemental carbon (EC), secondary inorganic aerosols (SIA) including SO_4^{2-}, NO_3^- and NH_4^+, mineral dust, and sea-salt.

The methodology for estimating the sea-salt and mineral dust fraction is the one proposed by Alastuey et al. (2016). Some elements such as Na, Mg, Ca and K are associated with both mineral dust and sea-salt aerosol. The sea-salt contribution was estimated for each element before estimating the mineral load. The concentrations of these elements in seawater are well known and therefore it is possible to estimate the marine contribution to PM mass once we know the concentration of one of these elements. Due to the potential volatilization of Cl by the interaction between NaCl with acidic species, the sea salt fraction of each species was estimated based on the concentration of marine Na. Thus, given that Na can be partially related to mineral dust, first, we calculated the mineral fraction of Na from the content of Al by using the ratio determined by (Moreno et al., 2006) for soils and dust in North Africa (the major source of dust in Southern Europe). Thus, the mineral sodium (non-sea-salt sodium, Na_{dust}) was obtained by multiplying Al concentration by 0.12, and the sea-salt fraction of Na (Na_{ss}) can be estimated by subtracting Na_{dust} from the total Na. The sea-salt fraction of calcium, magnesium, potassium and sulphate was estimated by using their seawater ratios concerning Na_{ss} (Nozaki, 1997). Finally, the total sea-salt load was determined by the sum of Cl^-, Na_{ss}, Ca_{ss}, Mg_{ss}, K_{ss} and $SO_4^{2-}{}_{ss}$. The non-sea-salt (nss) fractions of Ca, Mg, Mn, Na, K and SO_4^{2-} were obtained by subtracting the previously calculated sea-salt fraction from their bulk concentration. In addition to the sea salt fraction, K can be related to mineral (K_{dust}) and biomass burning (K_{bb}). The mineral fraction is estimated from Al ($K_{dust} = 0.31 \cdot Al$, (Moreno et al., 2006), and the biomass fraction by the difference: $K_{bb} = K - K_{ss} - K_{dust}$. Finally, the total mineral dust concentration was determined by addition of the concentrations of all mineral related elements expressed as oxides, such as Al_2O_3, SiO_2, Fe_2O_3, TiO_2, P_2O_5, CaO_{dust}, MgO_{dust}, Na_2O_{dust}, and K_2O_{dust}. Assuming the major presence of CaO_{dust} as CaCO3, the $CaCO_3$ was estimated from CaO_{dust} by multiplying by 1.274. This methodology can be only applied when the bulk concentrations of major elements (Al, Si, Ca, Mg, Fe, Na, K) is determined. Since the elemental concentration was determined from acidic digestion of the quartz filter by ICP methods Si was not determined and we estimated it from Al content by multiplying Al content by 3 (Alastuey et al., 2016). Organic matter (OM) or organic aerosol (OA) has been estimated from organic carbon (OC), applying a OM:OC factor of 1.8, a common practice with this coefficient generally deduced from AMS on line measurements.

RI-URBANS (www.RIURBANS.eu) is supported by the European Commission under the Horizon 2020 – Research and Innovation Framework Programme, H2020-GD-2020, Grant Agreement number: 101036245

2.4 Source apportionment analysis

2.4.1 Particulate Matter chemistry

Positive Matrix Factorization (PMF, Paatero and Tapper, 1994) is the most common receptor model used for source apportionment and it is based on the mass conservation principle:

$$x_{ij} = \sum_{k=1}^{p} g_{ik} f_{jk} + e_{ij} \quad i = 1, 2, \cdots, m \quad j = 1, 2 \cdots n$$

where x_{ij} is the concentration of the species j in the i^{th} sample, g_{ik} is the concentration of the k^{th} source in the i^{th} sample, f_{jk} is the contribution of the species j in source k and e_{ij} is the residual concentration. PMF can be solved with the Multilinear Engine (ME-2) developed by (Paatero, 1999) and implemented in the US EPA PMF v5. In this study, the US EPA PMF v5 (Norris et al., 2014) was applied to the three datasets independently. A harmonization method is applied to each dataset, including input chemical species, uncertainty calculation, result validation criteria, and implementation steps to ensure the homogeneity of PM source apportionment results. Input chemical species are chosen based on the well-known source tracers, as presented in various studies (Weber et al., 2019; Waked et al., 2014). In addition, organic species are added to identify sources of organic aerosols and elucidate the fate of these organics in the atmosphere (Borlaza et al., 2021; Glojek et al., 2024). The PMF input data for PM10 and PM2.5 source apportionment analysis are summarized in Table 3 and 4. The measurement uncertainty is important in the PMF model as its algorithm is based on the weighted least squares method, where uncertainty is considered as the weighting. Uncertainty is calculated using concentration and analysis error (Gianini et al., 2013), denoting that a species with higher uncertainty has less influence in the PMF model. See ST10 on PM source apportionment from RI-URBANS.

Criteria for validation were chosen based on European recommendations for using the receptor model (Mircea et al., 2020). These are: (1) low influence of data outliers based on the ratio of $Q_{true}/Q_{robust} < 1.5$. (2) The presence of trace species in the profile and the temporal evolution are clear enough to identify a source. (3) All factors should have a contribution > 1% to the total variable PM10. (4) The distribution of residuals from -3 to 3 indicates the absence of outliers and the feasibility of reconstruction. (5) The correlation coefficient between species concentration measured and predicted by PMF must be greater than 0.5. (6) Good bootstrap value: represents the stability of the solution: at least 70 runs per 100 runs, where the correlation between the base run and boot runs is greater than 0.6. For each data set, the PMF is run from 4 to 12 factors to observe the evolution of the chemical profile and contribution over the number of factors. For each run, the solution is attentively evaluated using the validation criteria. The results of the different inputs/number of factors are compared to determine the most appropriate solution.

RI-URBANS (www.RIURBANS.eu) is supported by the European Commission under the Horizon 2020 – Research and Innovation Framework Programme, H2020-GD-2020, Grant Agreement number: 101036245

Table 3. *PMF input variables for the PM10 analyses.*

Athens	**Barcelona**	**Paris**	**Zurich**
PM10 (total variable)	PM10 (total variable)	PM10 (total variable)	PM10 (total variable)
OC*, EC	OC*, EC	OC*, EC	OC*, EC
Cl^-, NO_3^-, SO_4^{2-}, Na^+, NH_4^+	Cl^-, NO_3^-, SO_4^{2-}, Na^+, NH_4^+, K^+	Cl^-, NO_3^-, SO_4^{2-}, Na^+, NH_4^+, K^+	Cl^-, NO_3^-, SO_4^{2-}, Na^+, NH_4^+, Mg^{2+}, Ca^{2+}
K, Mg, Ca, Al, Fe, Ti, V, Mn, Ni, Cu, Zn, Rb, Sn, Pb	Mg, Ca, Al, Fe, Ti, V, Cr, Mn, Ni, Cu, Zn, As, Rb, Sn, Sb, Pb	Mg, Ca, Al, Fe, Ti, V, Cr, Mn, Cu, Zn, As, Se, Rb, Sn, Sb, Ba, Pb	Al, Fe, Ti, V, Mn, Cu, As, Rb, Cd, Sn, Sb, Pb
Levoglucosan, Mannitol, 3-methylbutanetricarboxylic acid (3-MBTCA)	Levoglucosan, Arabitol+Mannitol, 3-MBTCA,	levoglucosan, Arabitol+Mannitol, methanesulfonic acid (MSA), 3-MBTCA, 2-Methylthreitol	levoglucosan, mannosan, Arabitol+Mannitol, 3-MBTCA, 2-Methylthreitol, Phthalic acid

OC refers to the amount of measured OC minus the amount of equivalent OC from organic markers also included in the PMF. PM mass concentrations are from TEOM/FIDAS.*
Elements with charges represent the water-soluble concentration measured by ion chromatography and elements without charges represent the total concentration measured by ICP.

Table 4.*PMF input variables for PM2.5 analyses.*

Barcelona	**Paris**	**Zurich**
PM2.5 (Total variable)	PM2.5 (Total variable)	PM2.5 (Total variable)
OC*, EC	OC*, EC	OC*, EC
Cl^-, NO_3^-, SO_4^{2-}, NH_4^+, Na^+	Cl^-, NO_3^-, SO_4^{2-}, NH_4^+, Na^+, K^+, Ca^{2+}	Cl^-, NO_3^-, SO_4^{2-}, NH_4^+, Na^+
K, Mg, Ca, Al, Fe, Ti, V, Mn, Ni, Cu, Rb, Sn, Sb, Pb	Mg, Al, Fe, Ti, V, Mn, Cu, Sn, Pb	K, Ca, Al, Fe, Ti, V, Mn, Cu, Zn, Rb, Sn, Sb, Pb
Polyols, Levoglucosan, 3-MBTCA	Polyols, Levoglucosan, 3-MBTCA, Phthalic acid	Levoglucosan, 3-MBTCA

OC refers to the amount of measured OC minus the amount of equivalent OC from organic markers also included in the PMF. PM mass concentrations are from TEOM/FIDAS.*
Elements with charges represent the water-soluble concentration measured by ion chromatography and elements without charges represent the total concentration measured by ICP.

2.4.2 Non-targeted mass spectral analyses of water-soluble organic carbon

Source apportionment based on the non-targeted mass spectral analyses was performed following the methodology proposed by Cui et al. (2024) relying on PMF - the same receptor model as for the source apportionment using the PM chemistry (section 2.4.1). From this analysis, we obtained chemical fingerprints and time series of water-soluble organic aerosol sources. The sources' contribution to organic carbon was determined in a second step via a multilinear regression.

RI-URBANS (www.RIURBANS.eu) is supported by the European Commission under the Horizon 2020 – Research and Innovation Framework Programme, H2020-GD-2020, Grant Agreement number: 101036245

2.4.3 Particle Number Size Distribution of ultrafine particles

Source apportionment of PNSD was performed following the methodology proposed by Garcia-Marlès et al. (2024b) relying on PMF - the same receptor model as for the source apportionment using the PM chemistry (section 2.4.1). Given the large datasets that cannot be handled by US EPA PMF, source apportionment was performed using the tool developed by Hopke et al. (2023) using ME-2. The datasets included hourly averaged PNSD data combined with hourly concentrations of the ancillary co-pollutants (eBC, PM_X, NO_2, NO, SO_2, O_3 and CO, when available), to help the identification of the sources. PMF requires individual uncertainty estimates for each data value. Detailed information about the estimation of uncertainties in the PNC and PNSD values is available in Garcia-Marlès et al. (2024b). See ST11 on UFP-PNSD source apportionment from RI-URBANS.

The datasets for each site were independently analysed by PMF. PMF was run multiple times for different numbers of factors (sources). Factor profiles and contributions that were obtained were plotted to explore their physical interpretability. If the results were not consistent, PMF was run again with a different number of factors. Then, the number of sources was finally determined, examining the results and choosing the best solution. The solutions were selected according to the accepted criteria and guidelines (Hopke et al., 2023; Belis et al., 2019), as described above for the chemistry PMF, considering: (i) scaled residuals approximately randomly distributed between -3 and 3, (ii) a Qtrue/Qexp ratio close to 1, (iii) profile uncertainties determined by the displacement (DISP) method, and (iv) the provision of the most physically meaningful profiles and temporal behaviours. To support the identification of the sources, the contributions of each factor to the variance of the co-located ancillary pollutants, daily patterns, seasonality, and polar plots were evaluated, and sources were identified using existing literature. The data analysis and plots were performed with the R statistical software (v4.2.3) and the package *Openair* (Carslaw and Ropkins, 2012). Source apportionment results from this study from 2020-2023 will be presented for Athens, Barcelona and Paris. Zurich was excluded from the study due to issues with data quality.

2.4.4 eBC

Aethalometer source apportionment analysis was performed between 2020 and 2023 to estimate the contributions of eBC emitted by combustion of liquid fuel (eBC_{LF}), mainly related to traffic exhaust emissions, and solid fuel (eBC_{SF}), mainly from residential and commercial wood burning, at four pilot sites using the Aethalometer model (Sandradewi et al., 2008). This model uses the 7- babs measurements provided by AE instruments and it is based on the fact that solid fuel sources emit eBC together with specific organic aerosols (OA) that can absorb in the UV-VIS spectral range (the so-called Brown Carbon, BrC) thus causing an increase of AAE. The model permits quantifying the contribution of BC emitted by combustion of liquid fuel (eBC_{LF}) and by combustion of solid fuel (eBC_{SF}). The results of the Aethalometer source apportionment model depend on the chosen Absorption Angstrom Exponent (AAE). Usually, two pairs of values are used: 1 and 2 for AAE_{LF} and AAE_{SF}, respectively (Sandradewi et al., 2008), and 0.90 and 1.68, respectively (Zotter et al., 2017). An alternative method involves using the frequency distribution of AAE to estimate site-specific values (Tobler et al., 2021). According to the GUIDANCE DOCUMENTS ON MEASUREMENTS & MODELLING OF NOVEL AIR QUALITY POLLUTANTS: Source apportionment of eBC, UFP, OP and VOCs (ST11), source-specific absorption AAEs for liquid (AAE_{LF}) and solid (AAE_{SF}) fuel combustion have been selected as the linear fit in a log-log space between the seven harmonized absorptions from AE instruments and the corresponding wavelengths. To do this, the 1st and 99th percentiles of the experimental AAE_{LF} and AAE_{SF} values were obtained respectively, for BC source apportionment. Only AAE values obtained from fits with R^2>0.99 were used to calculate the 1st percentile, whereas unfiltered AAE values were used to calculate the 99th percentile. Moreover, in order to minimize the contribution to absorption from BrC sources, the 1st percentile was calculated using summer absorption data. Conversely, and in order to maximize the contribution from BrC sources, winter data should be used to calculate the 99th percentile. For a detailed description of the eBC source apportionment, the related sensitivity study, and the recommendations, please refer to the RI-URBANS service tool document for eBC source

RI-URBANS (www.RIURBANS.eu) is supported by the European Commission under the Horizon 2020 – Research and Innovation Framework Programme, H2020-GD-2020, Grant Agreement number: 101036245

apportionment (https://riurbans.eu/wp-content/uploads/2024/07/ST2_BC.pdf). See ST11 on BC source apportionment from RI-URBANS.

2.4.5 Oxidative potential

The methodology for source apportionment of OP is also reported in ST11 on OP source apportionment from RI-URBANS. In brief, OP is apportioned to PM sources (post-PMF analysis) via a multilinear framework using the OP time series data as target and the PM sources concentration time series as predictors.

3 Results

All the analysis is completed, and the results are shared with the RI-URBANS partners at https://www.healthpilot-riurbans.eu/.

3.1 PM composition

Yearly mean PM10 concentrations were higher in Athens (32 µg m^{-3}), lower in Paris (23 µg m^{-3}) and Barcelona (22 µg m^{-3}), and lowest in Zurich (16 µg m^{-3}). PM2.5 concentrations were substantially lower but otherwise showed a similar spatial behaviour: Athens (24 µg m^{-3}), Barcelona (15 µg m^{-3}), Paris (11 µg m^{-3}), Zurich (11 µg m^{-3}). These values meet the requirements for the annual mean value set by the EU 2008/50/EC Directive for PM10 (40 µg m^{-3}) and PM2.5 (25 µg m^{-3}), but do not comply with the new directive EU 2024/2881/EC for 2030, (20 µgPM10 m^{-3} and 10 µgPM2.5 m^{-3}) except for PM10 in Zurich. The PM2.5 and PM10 chemical analyses of trace elements, water-soluble inorganic ions, organic and elemental carbon are used for reconstructing the gravimetrically determined mass concentration (Figure 3). The chemically reconstructed mass accounts for 75% in Barcelona, 86% in Paris, 91% in Athens, and 96% in Zurich. The lowest chemically reconstructed PM mass fraction in Barcelona can be related to higher humidity (and then to highest aerosol liquid water content) and/or to a higher contribution of secondary organic aerosols (SOA; with higher OM-to-OC ratio than expected) and/or loss of semi-volatile species (such as ammonium nitrate) during sampling. However, there is a good correlation between PM10 daily concentrations and total mass determined at all sites (Figure 4).

The main PM10 constituents are displayed in Figure 3. In Athens, with a drier climate and a more pronounced desert influence, dust is a larger contributor to PM10 than at the other locations. Secondary inorganic aerosol (SIA: sulphate, nitrate, ammonium) as well as Organic Matter (OM) are other substantial contributors to PM at all locations. We found that the organic carbon is to a substantial amount water-soluble without much variation between the pilot cities (Athens: 38%, Barcelona 43%, Paris 42%, Zurich 43%).

RI-URBANS (www.RIURBANS.eu) is supported by the European Commission under the Horizon 2020 – Research and Innovation Framework Programme, H2020-GD-2020, Grant Agreement number: 101036245

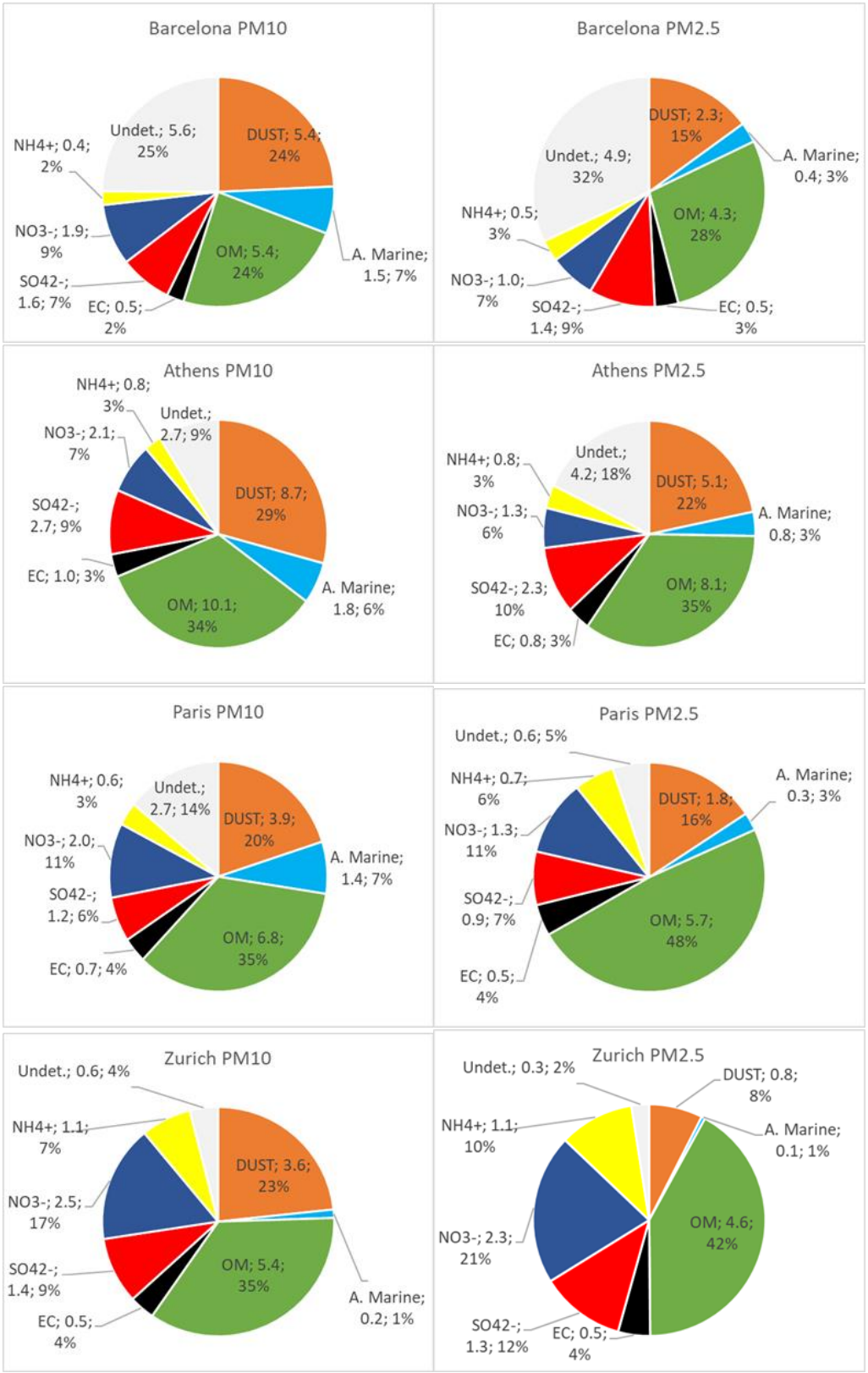

***Figure 3**. Average contribution of major groups of elements (Mineral dust; Marine aerosol; Organic matter, and SIA) for 4 pilot cities for PM_{10} (left column) and $PM_{2.5}$ (right column). Results in µg m-3.*

RI-URBANS (www.RIURBANS.eu) is supported by the European Commission under the Horizon 2020 – Research and Innovation Framework Programme, H2020-GD-2020, Grant Agreement number: 101036245

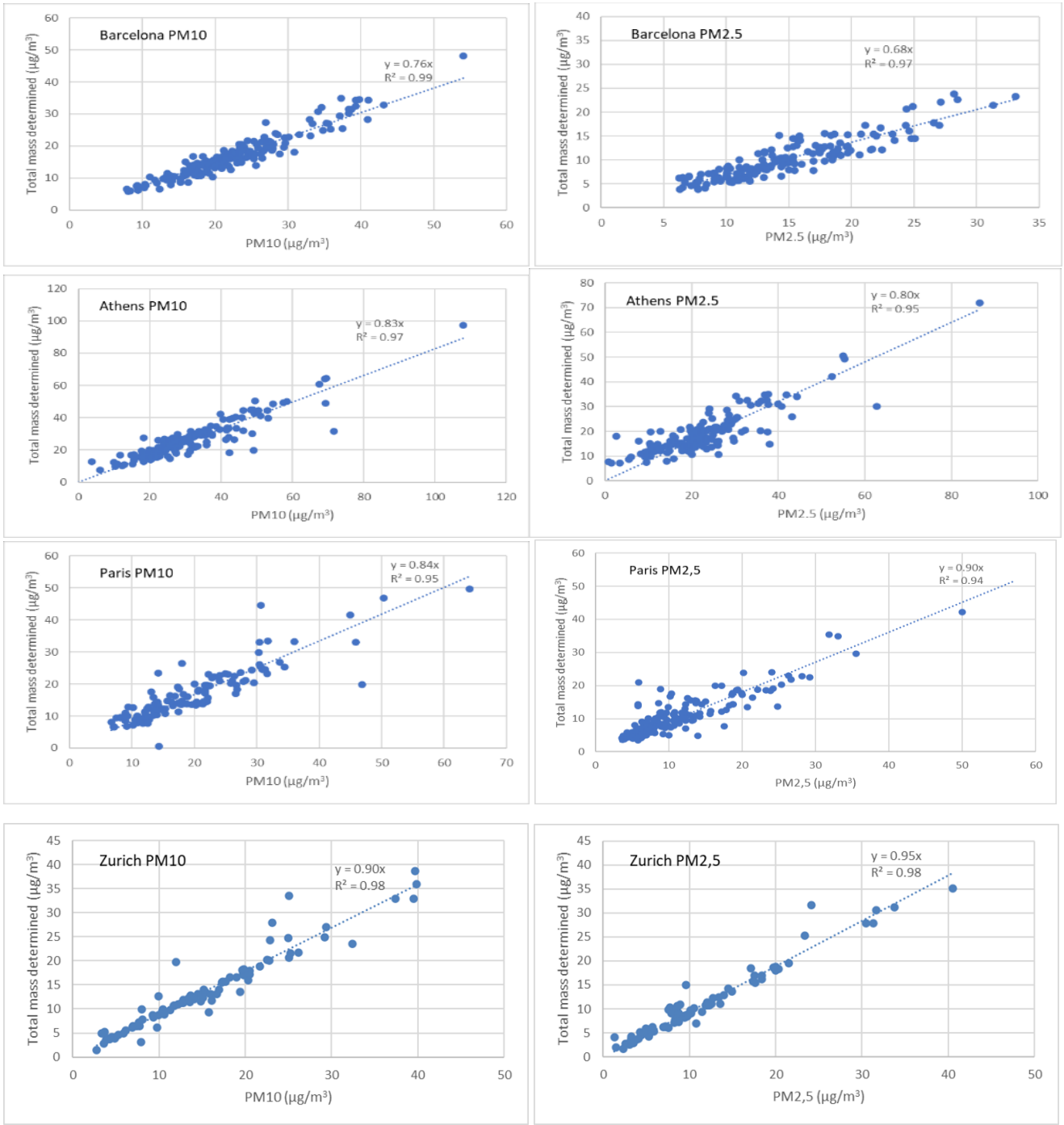

***Figure 4**. Scatter-plots showing correlations between daily PM10 concentrations and total mass determined per each filter (dust+marine aerosol+OM+EC+SIA) for 4 pilot cities for $PM_{2.5}$ (right column) and PM_{10} (left column).*

RI-URBANS (www.RIURBANS.eu) is supported by the European Commission under the Horizon 2020 – Research and Innovation Framework Programme, H2020-GD-2020, Grant Agreement number: 101036245

3.2 Brown carbon

The sites of Athens, Paris and Barcelona presented a yearly average BrC absorption coefficient ($Abs_{WS\_BrC\_365}$) of 2.04, 1.16, and 0.88 Mm^{-1}, respectively for fine aerosol (PM2.5); while the corresponding values for PM10 fractions were 2.59, 1.65, 0.99 Mm^{-1}, respectively. The city of Athens reveals the highest water-soluble BrC values, followed by Paris; while the city of Barcelona demonstrates the lowest values on a yearly basis. In the city of Zurich, an absorption coefficient of 0.90 Mm^{-1} was measured for fine aerosol fraction, while the respective water-soluble BrC absorption coefficient for PM10 was estimated at 1.03 Mm^{-1}; the latter values appear to be similar to the levels recorded in the city of Barcelona. It is worth noting that Athens and Paris have strong seasonal variations, presenting much higher values during winter, which is not the case for the other 2 studied cities of Barcelona and Zurich. The latter observation highlights some essential differences in the composition of OM in these former cities on a seasonal basis.

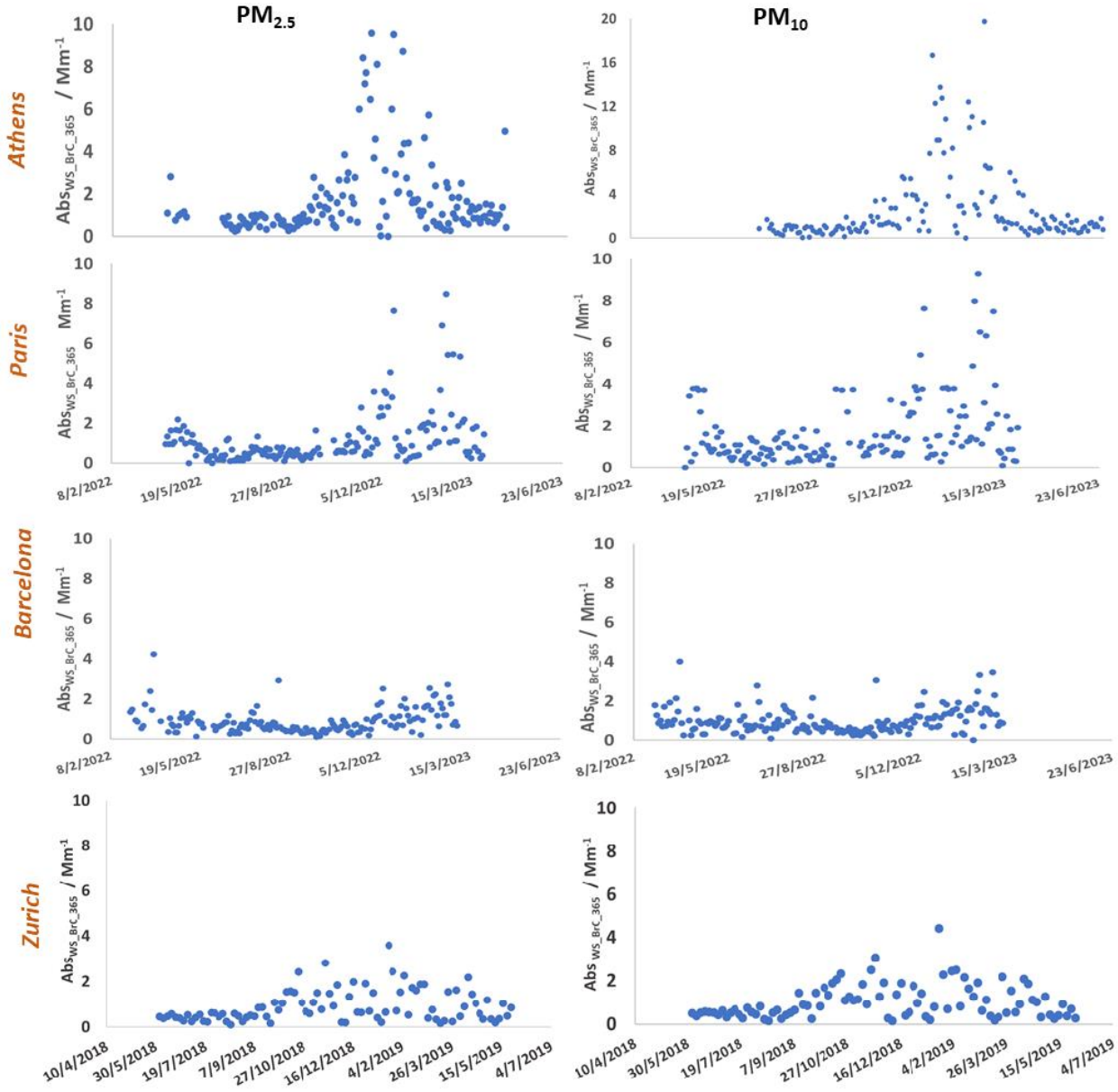

Figure 5. *Time-series (Feb 2022 – Jun 2023) of water-soluble brown carbon (BrC) analyses displayed as BrC absorption coefficient ($Abs_{WS\_BrC\_365}$) for all 4 pilot cities for $PM_{2.5}$ (left column) and PM_{10} (right column).*

RI-URBANS (www.RIURBANS.eu) is supported by the European Commission under the Horizon 2020 – Research and Innovation Framework Programme, H2020-GD-2020, Grant Agreement number: 101036245

Figure 6 shows the respective BrC $AAE_{365-590}$ values on a seasonal basis, for all studied cities. With regards to fine aerosol fraction ($PM_{2.5}$), in Zurich the mean seasonal BrC AAE ranged between 6.73 ± 1.1 (in spring) and 7.40 ± 0.81/1.20 (in summer / winter, respectively), presenting the highest values between the studied cities. Athens and Paris followed with mean values of 6.64 ± 0.51 and 6.63 ± 0.56, respectively; while Barcelona demonstrated slightly lower values, with an average AAE of 6.03 ± 0.37. Similar variance is observed between the 4 studied cities for PM_{10} aerosol fraction, as well. Zurich presented the highest mean value (7.02 ± 0.40), followed by Paris and Athens (6.49 ± 0.53 & 6.09 ± 0.77, respectively), and finally in Barcelona, the mean BrC AAE value was calculated at 5.94 ± 0.54. All estimated values appear to be higher than 4 during the whole year, indicating that water-soluble BrC in the four studied cities is variably impacted by both local combustion sources and secondary aerosol processing (Paraskevopoulou et al., 2023).

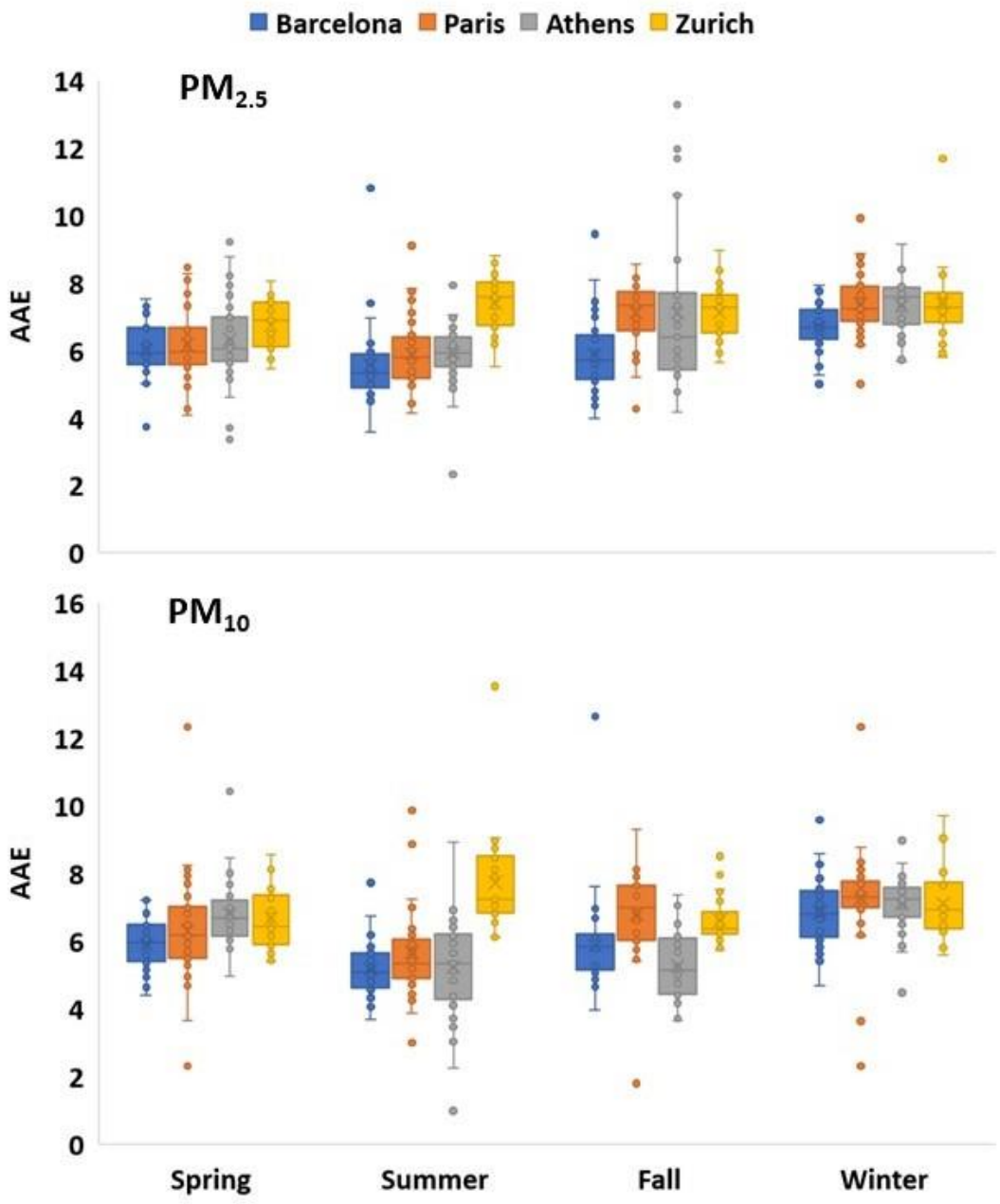

Figure 6. *Whisker plots summarizing data of water-soluble brown carbon (BrC) analyses on a seasonal basis, displayed as absorption Ångström exponent (AAE), for all 4 pilot cities for $PM_{2.5}$ (top plot) and PM_{10} (bottom plot).*

RI-URBANS (www.RIURBANS.eu) is supported by the European Commission under the Horizon 2020 – Research and Innovation Framework Programme, H2020-GD-2020, Grant Agreement number: 101036245

3.3 Source apportionment analyses based on PM chemistry

A unified source apportionment analysis has been performed for each of the pilot cities. In order to devise this PMF strategy, we performed a sensitivity assessment using two contrasting environments (Barcelona, Spain vs. Paris, France). Based on that, we performed source apportionment of PM10 in Athens, Barcelona, Paris, and Zurich and for PM2.5 for all cities but Athens. In brief, the PMF input includes the PM mass concentration, trace elements, water-soluble ions, elemental carbon and organic carbon, as well as organic marker compounds for primary wood burning PM (levoglucosan), primary biological PM (polyols), and secondary biogenic PM (e.g. 3-MBTCA) (Table 3). For all pilot sites, similar sets of PM sources were identified. Overall, we were able to quantify the following identified 11 PM sources: dust, primary biological, biomass burning, nitrate-rich, sulfate-rich, traffic, heavy fuel oil (HFO), secondary biogenic, MSA-rich, sea salt, aged sea salt. Most of these PM sources represent a mixture of primary and secondary constituents. The source contributions to PM are shown in Figure 7.

While most sources are present at all pilot cities, certain source categories are only identified in some of the pilot cities, e.g. HFO only in Athens and Barcelona likely due to the close proximity of major ports or MSA-rich only in Paris since the main marker MSA is not available at other pilots. Similarly, the impact of sea salt and aged sea salt together shows a clearly lower contribution in Zurich compared to the other pilot cities that are more strongly affected by marine air masses. On the other hand, the relative contribution of dust shows considerable variability between the pilots, which appears though not directly linked to the proximity of transported dust sources. Traffic is a major contributor to PM at all pilot cities and encompasses both the exhaust emissions (primary and formed secondary) as well as non-exhaust emissions. Overall, the impact of biomass burning on PM is smaller on a yearly basis than that of traffic at all pilots, but it can be dominant during the winter season. Nitrate-rich and sulfate-rich factors represent for the most part secondary inorganic PM but also include secondary organic carbon and some transported trace elements. Both of these factors are important contributors to PM at all pilots. In Paris and Zurich, there is more nitrate-rich per sulfate-rich PM than in Athens and Barcelona. This is likely related to thermodynamics favoring nitrate and similarly volatile constituents to reside in the particle phase in the more temperate climate in Paris and Zurich. Secondary biogenic organic aerosol is an important contributor in the mediterranean cities probably related to higher temperature favouring biogenic emissions of precursors. This factor also shows a strong seasonal variation.

RI-URBANS (www.RIURBANS.eu) is supported by the European Commission under the Horizon 2020 – Research and Innovation Framework Programme, H2020-GD-2020, Grant Agreement number: 101036245

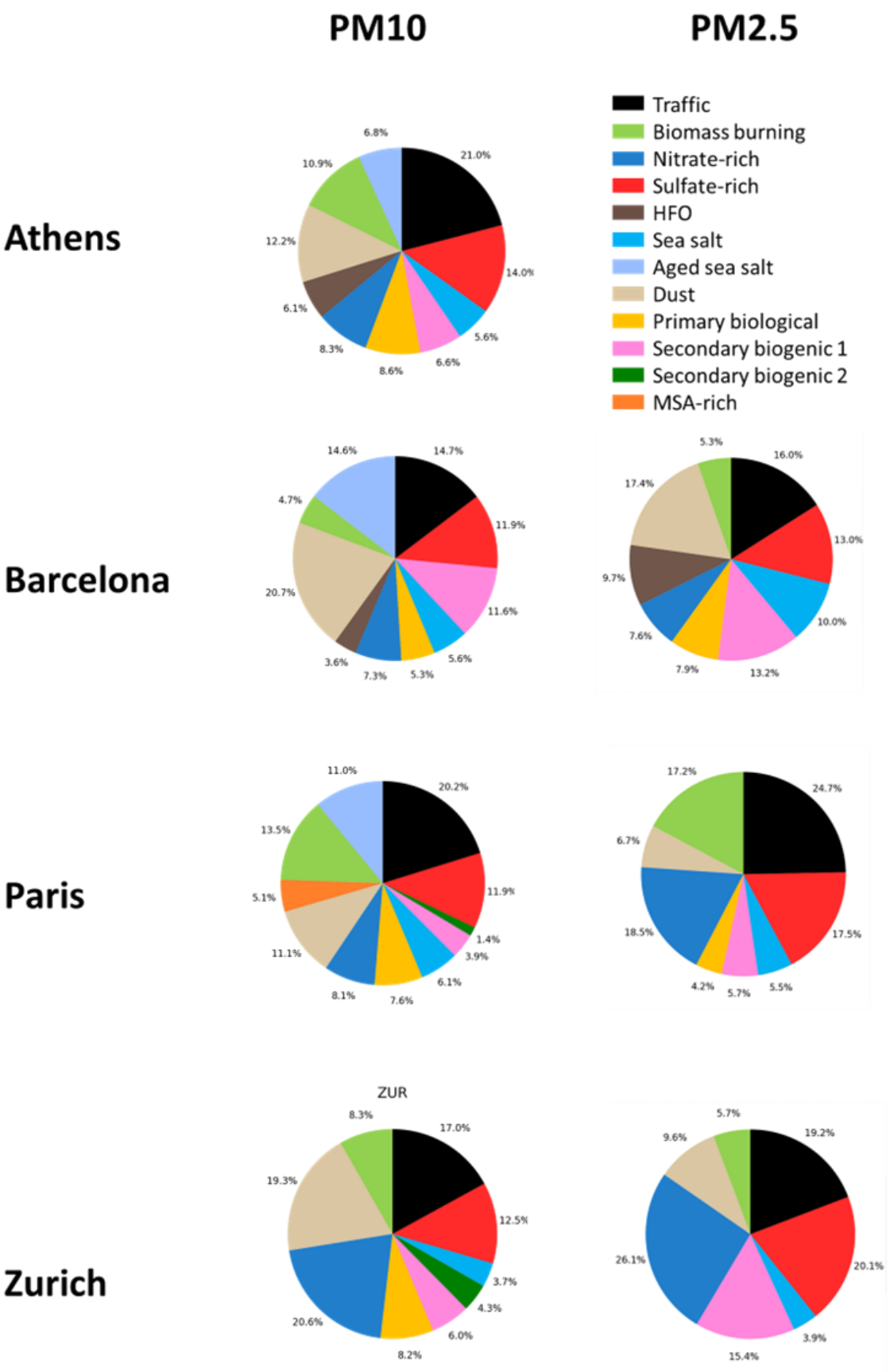

***Figure 7**: Particulate Matter sources in pilot cities (Athens, Barcelona, Paris, Zurich) for the two size fraction of the PM.*

RI-URBANS (www.RIURBANS.eu) is supported by the European Commission under the Horizon 2020 – Research and Innovation Framework Programme, H2020-GD-2020, Grant Agreement number: 101036245

3.4 Source apportionment of organic carbon via non-targeted mass spectral analyses

A source apportionment analysis has been performed for the organic carbon contained in particulate matter at all pilots based on the non-targeted mass spectral analyses of water-soluble carbon (see 2.3.8.). The source contributions to OC are shown in Figure 8 for Athens, Barcelona, Paris, and Zurich.

Since hydrocarbon-like organic carbon related to the combustion of liquid fossil fuels (e.g. road traffic) are largely water-insoluble their concentration was estimated based on collocated online eBClf analyses (see methods). All other identified OC types were measured as water-soluble fractions for which the water-solubility was determined empirically via a multilinear regression (see methods), while the unexplained OC fraction is termed “other OC”.

As a frontrunner, samples from Zurich were analysed with an Aerosol Mass Spectrometer that measures the organic molecules as fragment ions given the hard ionization pathway. Nevertheless, different types of OC could be quantified. Given the limited chemical information from the AMS, the samples from all other cities (Athens, Barcelona, Paris) were analyzed with a non-targeted extractive electrospray ionization mass spectrometer (EESI-MS). Water-soluble OC types were quantified with regard to their organic carbon concentration via a multilinear regression approach (see methods). With this approach, groups of largely similar OC quasi molecular types were identified, though with added chemical information obtained from tracer measurements on the same samples, facilitating relating the OC types to sources.

We find that emissions of the biosphere are represented in the 4 pilot cities by coarse primary biological OC (PBOC), related to pollen and spores, and secondary biogenic OC (much more in the PM2.5 fraction), related to oxidation products of biogenic volatile organic compounds such as alpha-pinene. In Athens, Barcelona, and Zurich biogenic SOC contribute roughly equally to OC, while in Paris the contribution is somewhat reduced. Given the local nature of coarse PBOC, a larger variability in the contribution of PBOC is observed, yet showing that PBOC is also a considerable contributor to coarse OC in urban areas. The impact of biomass burning emissions is in Athens and Paris larger than in Barcelona (and explain the variability in BrC properties in these 2 pilots). At first sight, the impact of such emissions in Zurich is comparable to Barcelona. However, anthropogenic SOC (aSOC) likely contains a contribution of SOC from biomass burning vapours that are represented at the other locations by a separate specific aged biomass burning OC or biomass burning SOC factor. In all pilots, a nitrogen-containing organic factor contributes to OC (NOC). While NOC shows chemical characteristics that could be consistent with cigarette smoke (e.g. C10H14N2 could be nicotine), the temporal variation (e.g. correlation with eBCf) suggests a major contribution from liquid fossil fuel combustion sources. In Paris, an additional OC type is identified that is correlated with water-soluble calcium. Likely, this OC type is related to local dust emissions close to the sampling location.

RI-URBANS (www.RIURBANS.eu) is supported by the European Commission under the Horizon 2020 – Research and Innovation Framework Programme, H2020-GD-2020, Grant Agreement number: 101036245

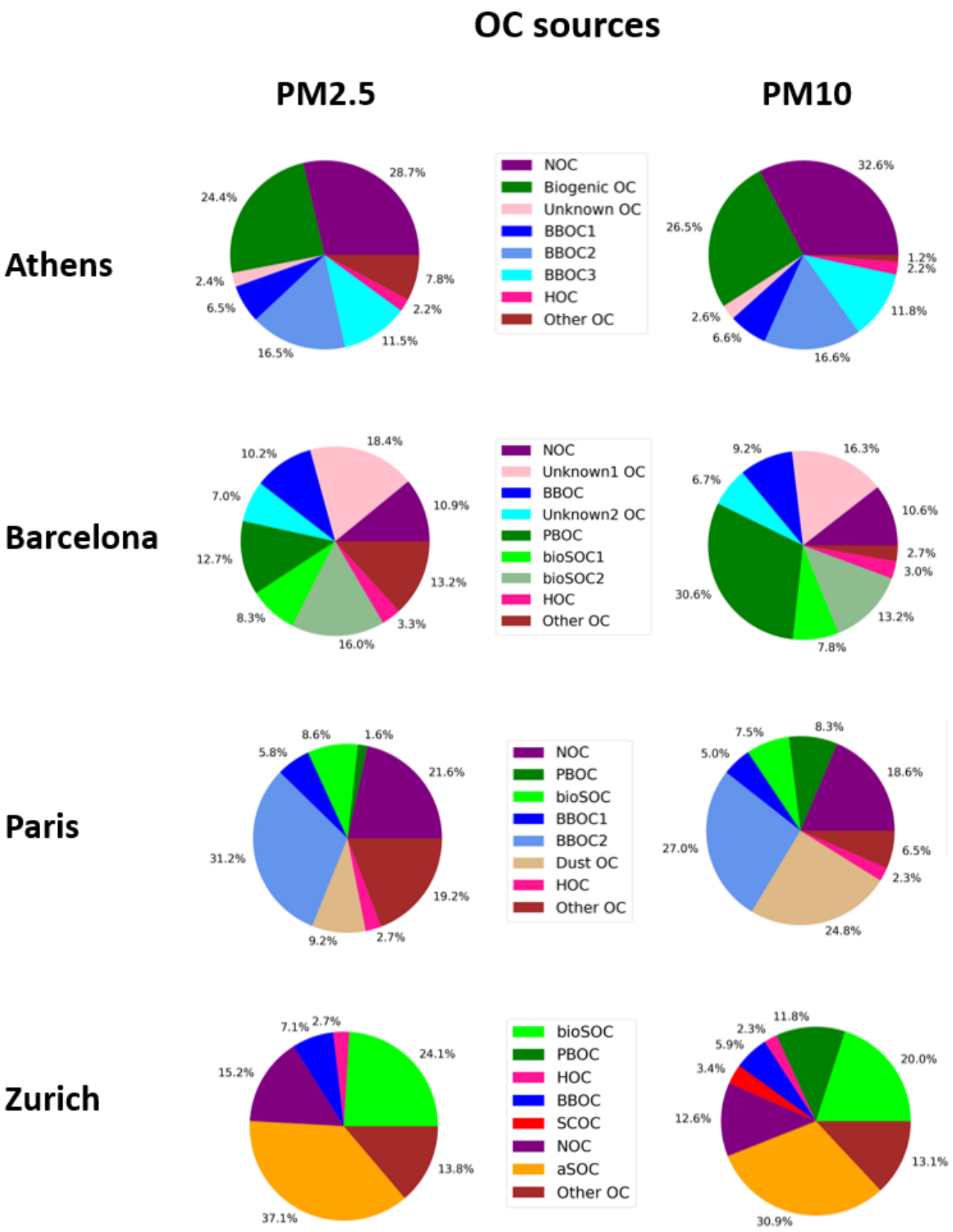

***Figure 8**. Sources of organic carbon. Results are based on non-targeted mass spectral analyses of water-soluble organic carbon (EESI-MS for Barcelona, Athens, Paris, AMS for Zurich).*

RI-URBANS (www.RIURBANS.eu) is supported by the European Commission under the Horizon 2020 – Research and Innovation Framework Programme, H2020-GD-2020, Grant Agreement number: 101036245

3.5 Source apportionment based on eBC data

Data on the eBC mass concentrations as well as the contribution of liquid (eBC_{LF}) and solid fuels (eBC_{SF}) are available at the RI-URBANS shared folder AE33. In this section, we present a summary of the eBC data collected at 4 pilot cities over the period from **2020 to 2023**. eBC mass concentrations were overall highest in Athens, followed by Barcelona and Zurich, and lowest in Paris. As described in the methodology section, and following ST11 recommendations we estimated AAE_{LF} and solid AAE_{SF} from the 1st and 99th percentiles of the experimental AAE_{LF} and AAE_{SF} values. Figure 9 shows the calculated AAE_{LF} and AAE_{SF} values effectively differentiating emission sources, with regional factors influencing their distributions.

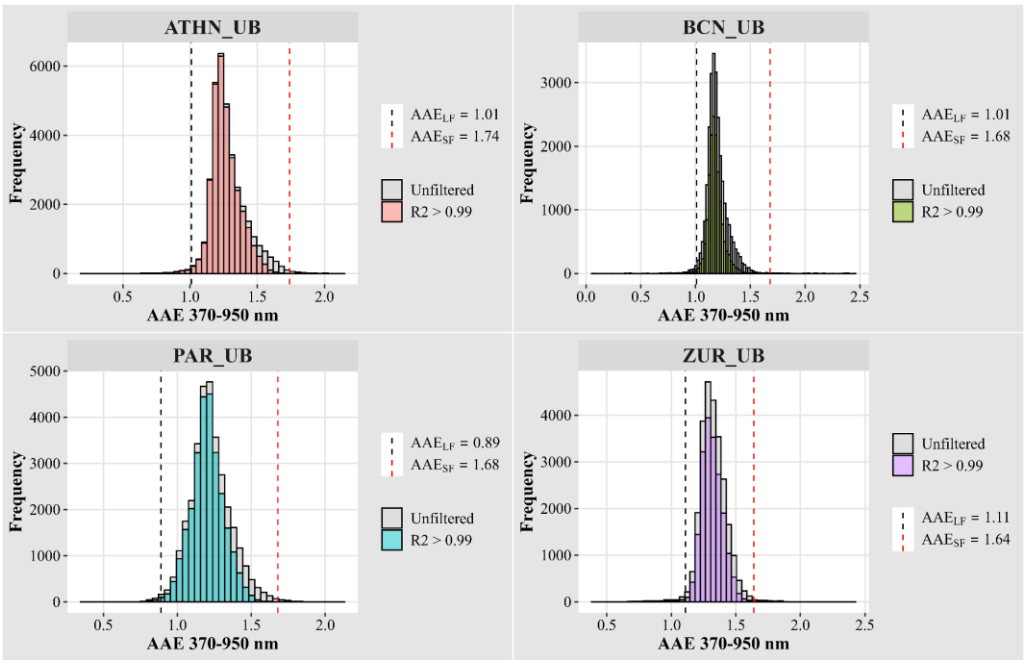

Figure 9. *Frequency distribution of absorption Ångström exponent (AAE) values calculated from Aethalometer data (370–950 nm) for pilot sites. The distributions are differentiated into* ***unfiltered AAE values*** *and* ***filtered AAE values with*** R^2*> 0.99. Credit to Savadkoohi et al. (2025, manuscript under review).*

Figure 10 shows variability in the relative contributions of eBC sources among the sites. The results indicate that fossil fuel combustion is the dominant source of eBC emissions in all four sites, with contributions ranging from 54.5% (Paris) to 67.0% (Barcelona). Solid fuel combustion varies significantly, with Paris exhibiting the highest contribution (45.5%), Athens (39.5%), Zurich (38.4%), and Barcelona the lowest (33.0%). The observed source variability highlights the influence of site-specific sources and regional atmospheric conditions. For instance, the relatively higher contribution of solid fuel combustion in Paris may reflect increased biomass burning activities (with log wood still being more used than pellets in France, especially compared to Switzerland, for instance), particularly during colder months, whereas the dominance of fossil fuel combustion in Barcelona aligns with traffic emissions.

RI-URBANS (www.RIURBANS.eu) is supported by the European Commission under the Horizon 2020 – Research and Innovation Framework Programme, H2020-GD-2020, Grant Agreement number: 101036245

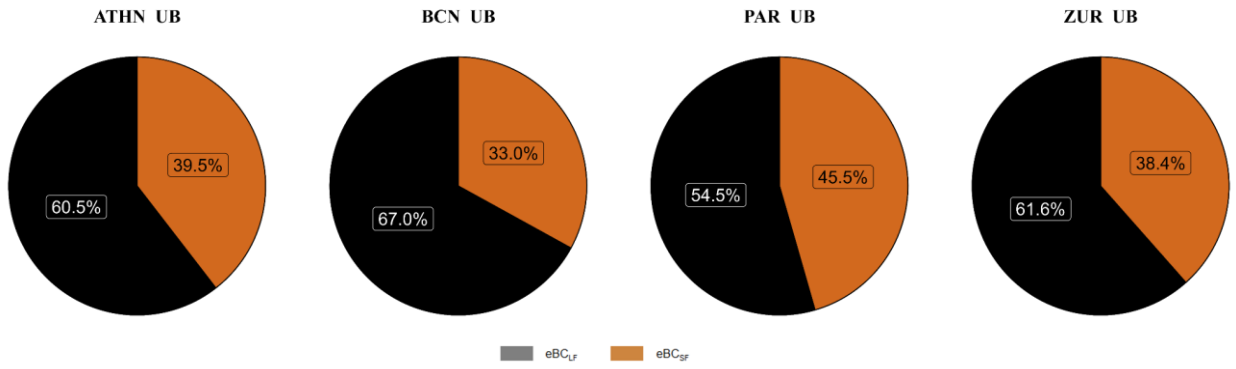

Figure 10. *Relative contribution of sources to total eBC at four pilot sites.*

As shown in Figure 11, at ATHN-UB and BCN-UB, eBC$_{LF}$ shows pronounced peaks during the morning and evening rush hours, indicative of traffic emissions. BCN-UB shows relatively stable patterns with lower solid fuel contributions compared to ATHN-UB where the evening peak in eBC$_{SF}$ suggests BB contributions or residential heating, common during evening hours. PAR-UB shows a more uniform diurnal variability for both sources. ZUR-UB shows a different pattern with a higher evening peak for eBC$_{SF}$, driven by residential heating and BB activities. Overall, the contribution of eBC$_{SF}$ varies across the sites but is generally lower than that of eBC$_{LF}$.

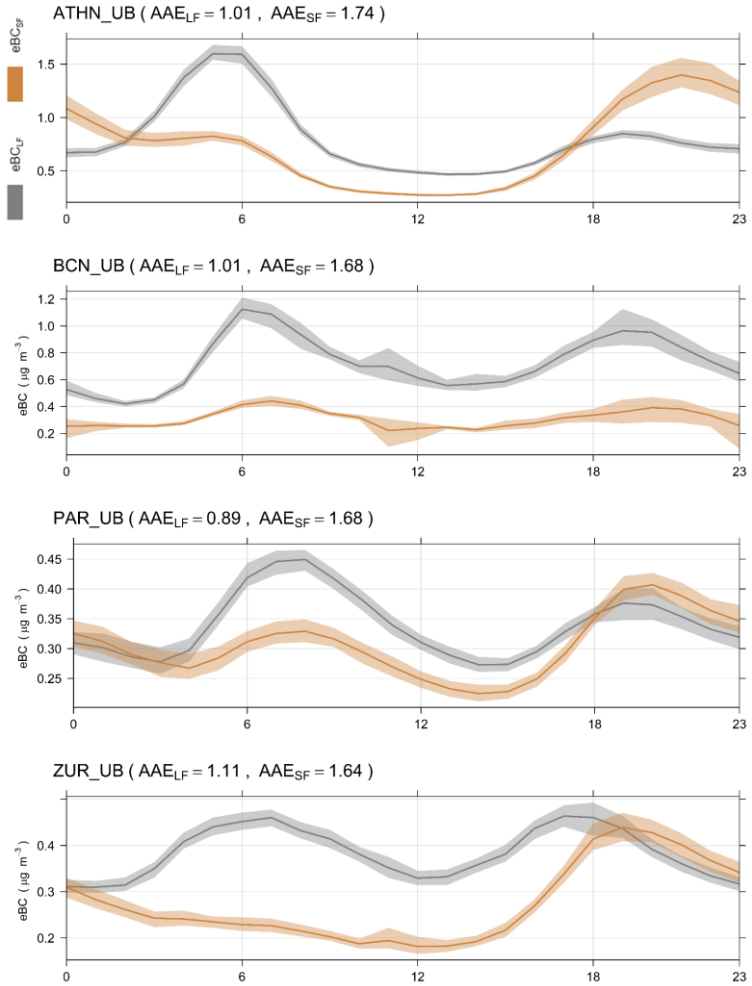

Figure 11. *Diurnal variations in liquid fuel combustion and solid fuel combustion for the four pilot monitoring sites.*

RI-URBANS (www.RIURBANS.eu) is supported by the European Commission under the Horizon 2020 – Research and Innovation Framework Programme, H2020-GD-2020, Grant Agreement number: 101036245

3.6 OP and its sources

A summary of the OP^{DTT} analysis is presented in this section for Athens, Barcelona, Paris, and Zurich (Figure 12). The yearly average oxidative potential of PM10 is the highest in Athens (2.6 nmol $min^{-1}m^{-3}$), followed by Paris (1.9 nmol min^{-1} m^{-3}) and Barcelona (1.8 nmol $min^{-1}m^{-3}$), and the lowest in Zurich (1.3 nmol $min^{-1}m^{-3}$). While for Athens a strong seasonal variation is apparent, this is not the case for other sites. On the other hand, in all pilot cities the oxidative potential is substantially higher in PM10 than in PM2.5, highlighting the importance of coarse particles for OP. The OP data generated here are discussed within the context of the largest database in Europe (Tassel et al., in review).

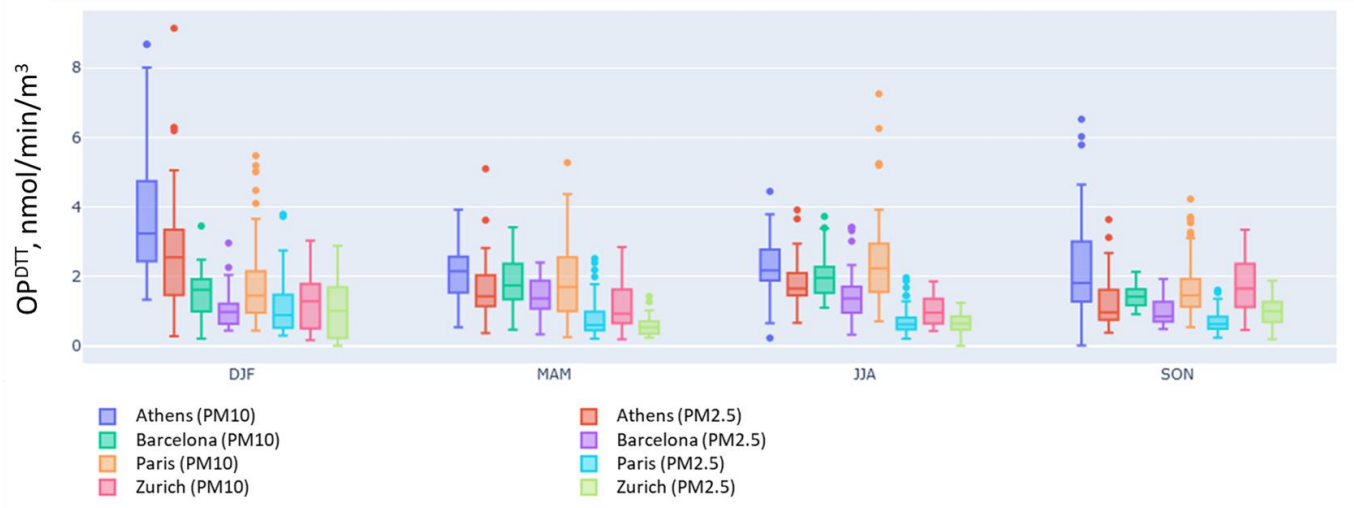

Figure 12. *OP^{DTT} (nmol/min/m^3) for the 4 cities separated by size fraction and season (DJF: December-January-February, MAM: March-April-May, JJA: June-July-August, SON: September-October-November): median, 1st and 3rd quartile as well as the upper and lower fence. This Figure is generated by https://www.healthpilot-riurbans.eu.*

For each pilot city, an OP source apportionment analysis was conducted for the two OP assays measured (OP^{DTT} and OP^{AA}). Where PM10 and PM2.5 source analyses are presented (only PM2.5 in progress for Athens), the OP source apportionment was performed independently for each PM size fraction. The findings reveal consistent intrinsic OP coefficients (ie OP per mass unit of PM, indicative of the nature of the PM) across all locations, falling largely within the variability observed in a previous analysis for France (Figure 13). Across all pilot cities, traffic emerges as the largest contributor to $OP^{DTT}$of PM10. Additionally, biomass burning, secondary PM linked to biogenic VOCs, and nitrate- and sulfate-rich PM are significant contributors. Dust also plays a key role in OP^{DTT} of PM10, but its contribution diminishes substantially in OP^{DTT} of PM2.5 due to the predominantly coarse nature of dust particles. A similar pattern of PM sources driving OP^{AA} is observed. For OP^{AA} of PM10, traffic is the dominant contributor in Barcelona, Paris, and Zurich, while biomass burning leads in Athens, with traffic being the second-largest contributor.

When examining the PM sources responsible for at least 80% of OP^{DTT} of PM10, traffic and dust are consistently identified in all four pilot cities (Figure 14). Biomass burning, aged sea salt, and sulfate-rich PM are present in two cities each, while nitrate-rich and bioSOA are identified in one city each. For OP^{AA} of PM10, traffic remains the only persistent source identified across all four locations, followed by sulfate-rich PM in three cities, heavy fuel oil (HFO) and biomass burning in two, and bioSOA, aged sea salt, and dust in one city each.

This analysis underscores the significant role of traffic emissions in driving OP for both DTT and AA assays. However, the relative importance of traffic exhaust and non-exhaust emissions remains unclear due to the inability to distinguish them in this analysis. Previous studies (Daellenbach et al., 2020) suggest that both exhaust and non-

RI-URBANS (www.RIURBANS.eu) is supported by the European Commission under the Horizon 2020 – Research and Innovation Framework Programme, H2020-GD-2020, Grant Agreement number: 101036245

exhaust emissions substantially influence OP. With non exhaust emissions being largely in the coarse mode PM, this is in line with a quite higher OP related to traffic in PM10 than PM2.5 for all pilots where both PM2.5 and PM10 OP source analyses are available. Similarly, the contribution of biomass burning PM likely encompasses both primary emissions and secondary PM, with prior research indicating that secondary biomass burning aerosols exhibit higher intrinsic OP than primary emissions. For nitrate-rich and sulfate-rich PM, the negligible intrinsic OP of pure ammonium nitrate (NH_4NO_3) and ammonium sulfate ($(NH_4)_2SO_4$) (already published in Daellenbach et al. 2020 for pure components) suggests that their contribution to OP is likely driven by other associated constituents, such as trace elements or secondary organic carbon. These findings highlight the complexity of PM composition and its influence on oxidative potential, emphasizing the need for further research to elucidate the specific drivers behind these factors.

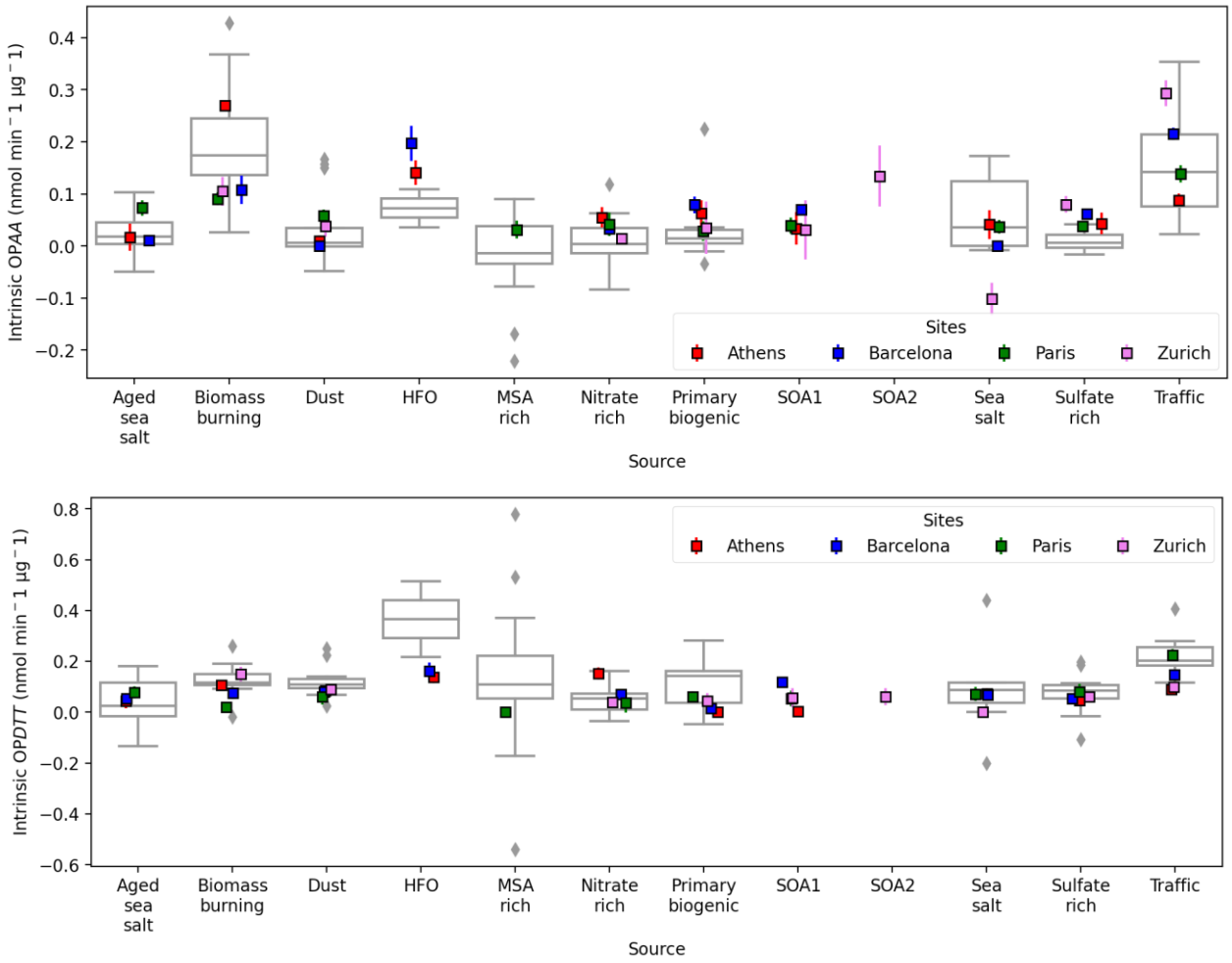

Figure 13. *Intrinsic OP coefficients (OPm, nmol/min/ug PM source) of all PM sources identified for PM10. Results from all pilots are compared to source-specific intrinsic OP coefficients from a previous study in France(indicated in grey) (Weber et al., 2021).*

RI-URBANS (www.RIURBANS.eu) is supported by the European Commission under the Horizon 2020 – Research and Innovation Framework Programme, H2020-GD-2020, Grant Agreement number: 101036245

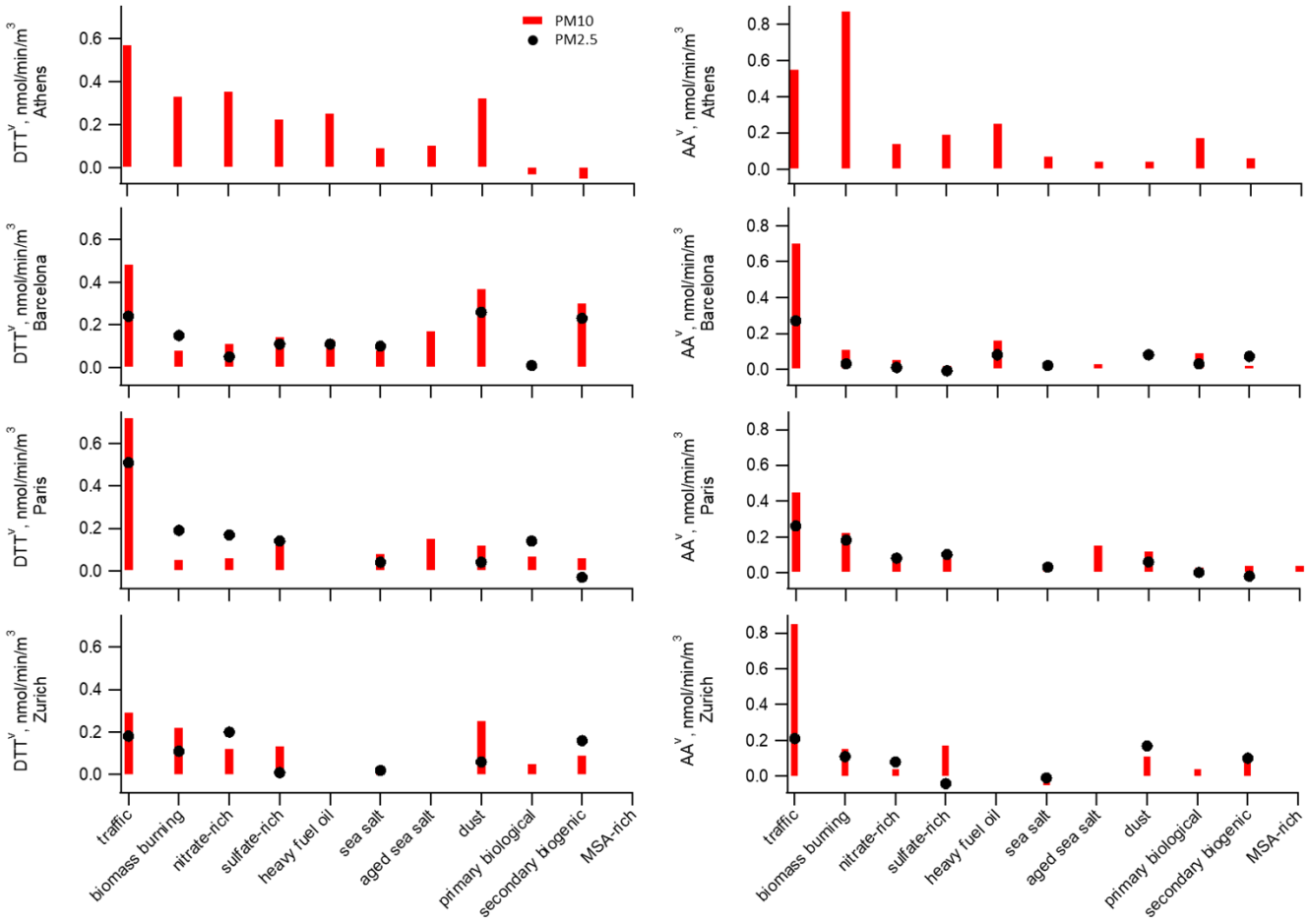

Figure 14. PM sources' contribution to oxidative potential (OPv, nmol $min^{-1}m^{-3}$) measured by the DTT and AA assay.

3.7 Source apportionment of UFP-PNSD

From the four pilot cities we report data and source apportionment for three of them (Athens, Barcelona and Paris). Source apportionment was not performed for Zurich due to dataset inconsistencies. The pilot measurements yielded results very similar to those from the 2017-2019 data compilation presented in previous reports (D2 (D1.2), García-Marlès et al., 2024a and b).

In Barcelona, the average concentrations of PNC were much lower for 2020-2023 (8355 # cm^{-3}) compared to 2017-2019 (11185 # cm^{-3}). However, the percentages of the Nucleation, Aitken, and Accumulation mode size fractions remained similar in both periods (38%, 50%, and 12% from 2017-2019, respectively; and 42%, 46%, and 12% from 2020-2023, respectively). In Athens, average PNC concentrations also decreased, from 8552 # cm^{-3} in 2017-2019 to 6908 # cm^{-3} in 2020-2022. The percentages of the Nucleation, Aitken, and Accumulation mode size fractions were also very similar in both periods (18%, 62%, and 20% from 2017-2019, respectively; and 18%, 60%, and 22% from 2020-2022, respectively). In Paris, the average concentrations of PNC from 2020-2023 were 9039 # cm^{-3} and the percentages of the Nucleation, Aitken, and Accumulation mode size fractions were 41%, 49%, and 10%, respectively. These cannot be compared to 2017-2019 because PNSD was not measured for this period.

Figure 15 shows that Barcelona continues to record high UFP in the Nucleation mode fractions, while Athens has higher concentrations in the Aitken mode, as reported in previous reports, probably due to the low NH_3

RI-URBANS (www.RIURBANS.eu) is supported by the European Commission under the Horizon 2020 – Research and Innovation Framework Programme, H2020-GD-2020, Grant Agreement number: 101036245

concentrations in the Athens region (Garcia-Marlès et al., 2024b). Paris has higher concentrations in the range between the Nucleation and the Aitken modes. Figure 16 shows the marked seasonal pattern of UFP in Athens and the parallelism with that of BC, with the highest concentrations occurring during traffic rush hours and lower values for both PNC and BC in summer. However, Barcelona exhibited a midday PNC peak in addition to rush hour peaks, with no clear seasonal patterns observed for either BC or PNC. Decreasing concentrations of both PNC and BC were recorded during weekends in Barcelona, but this was not seen in Athens. The results from 2020-2023 at both sites were consistent with those from the 2017-2019 period. Paris exhibited the highest PNC concentrations during traffic rush hours, similar to BC, and lower PNC concentration in summer, although BC does not display a seasonal pattern.

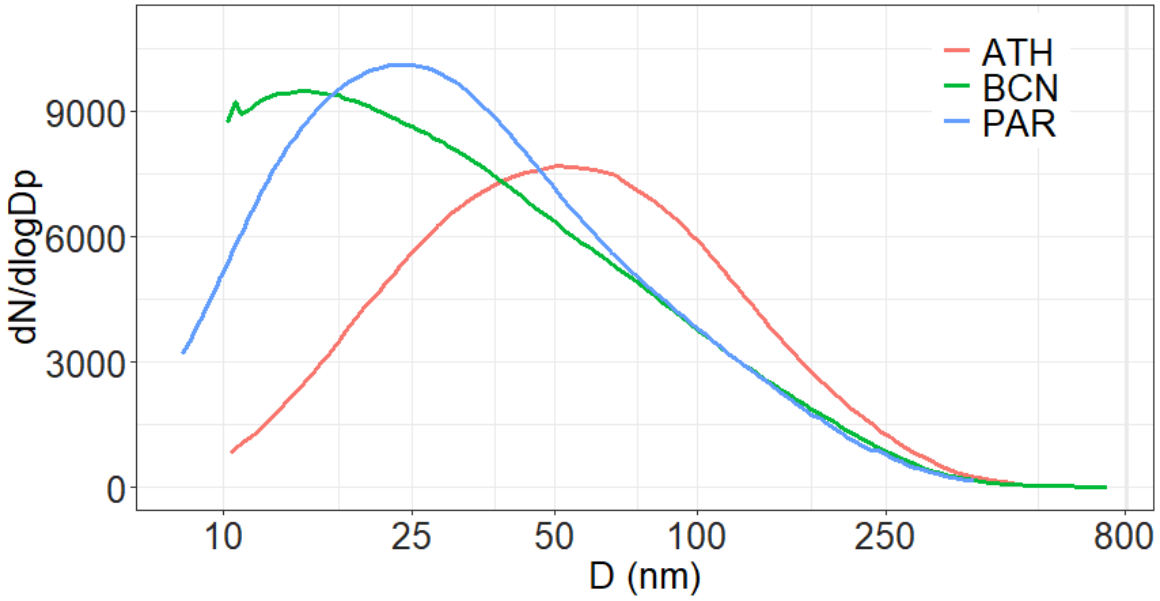

Figure 15: *Averaged Particle Number Size Distributions for Athens (ATH), Barcelona (BCN) and Paris (PAR) from 2020 to 2023.*

RI-URBANS (www.RIURBANS.eu) is supported by the European Commission under the Horizon 2020 – Research and Innovation Framework Programme, H2020-GD-2020, Grant Agreement number: 101036245

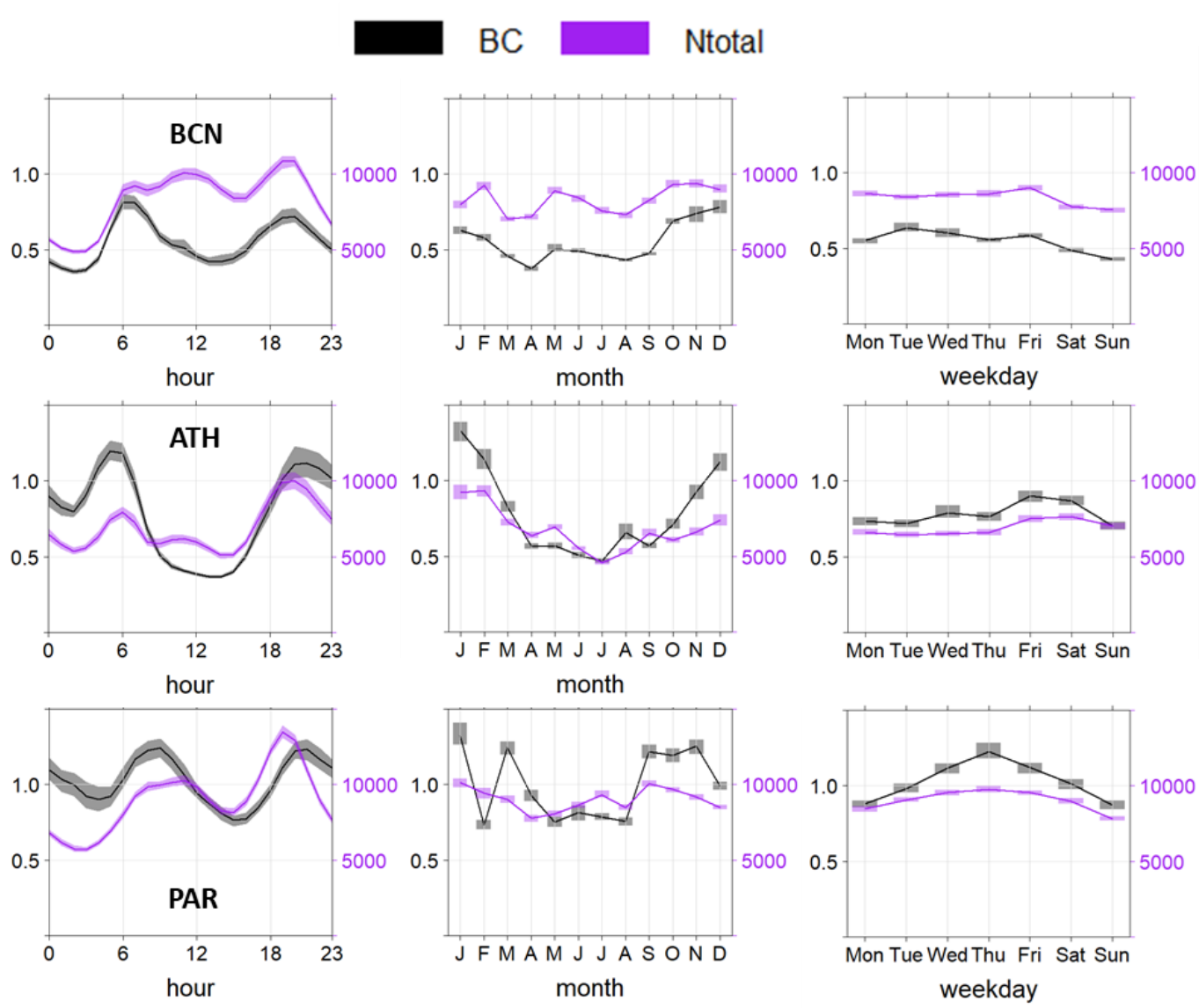

Figure 16. *Averaged hourly concentrations of Particle Number Concentration (Ntotal) and Black Carbon (BC) for Barcelona (BCN), Athens (ATH) and Paris (PAR) from 2020 to 2023. Particle Number Concentration is expressed in # cm^{-3}, and BC in µg m^{-3}.*

Figure 17, 18, and 19 show the source apportionment results for Barcelona, Athens, and Paris, respectively, where six sources were identified at all three sites.

In Barcelona, three traffic-related factors were identified, characterised by high PNC concentrations during traffic rush hours and lower values on weekends. *Traffic-1*, with a primary size mode at 25-30 nm, contributed 26% to the total PNC. It is associated with gasoline emissions (Ogulei et al., 2007; Liu et al., 2014; Hopke et al., 2022, 2024) and the nucleation of particles generated during the dilution of diesel exhaust semi-volatile organic compounds (SVOCs) (Harrison et al., 2011, Damayanti et al., 2023). This factor also exhibited a peak at midday, linked to the photonucleation of particles. *Traffic-2*, with a primary size mode at 80 nm, accounted for 16% of the total PNC and showed high contributions to the variance of NO2. It is associated with primary diesel vehicle emissions (Ogulei et al., 2007; Liu et al., 2014; Hopke et al., 2022). *Mixed traffic* is characterised by size mode peaks between those of *Traffic-1* and *Traffic-2*, representing a combination of traffic sources along with other emissions. *Photonucleation* exhibited a primary size mode at 15 nm, contributing to 28% of the total PNC. It displayed a pronounced midday

RI-URBANS (www.RIURBANS.eu) is supported by the European Commission under the Horizon 2020 – Research and Innovation Framework Programme, H2020-GD-2020, Grant Agreement number: 101036245

peak, linked to photochemically induced new particle formation (NPF) events, which are enhanced by strong solar radiation (Kulmala and Kerminen, 2008; Brines et al., 2015). Two regional sources were also identified at this site, both with peaks in the accumulation mode. *Regional-1* contributed 2% of the total PNC and is associated with nitrates formed primarily through atmospheric oxidation of NOX, predominantly during winter and at night (Dall'Osto et al., 2009; Masiol et al., 2016; Seinfeld and Pandis, 2016). *Regional-2* accounted for 5% of the PNC and is associated with secondary ammonium sulphate and organic aerosols, which are enhanced during summer and at midday, due to higher levels of solar radiation and ozone (Ehn et al., 2014).

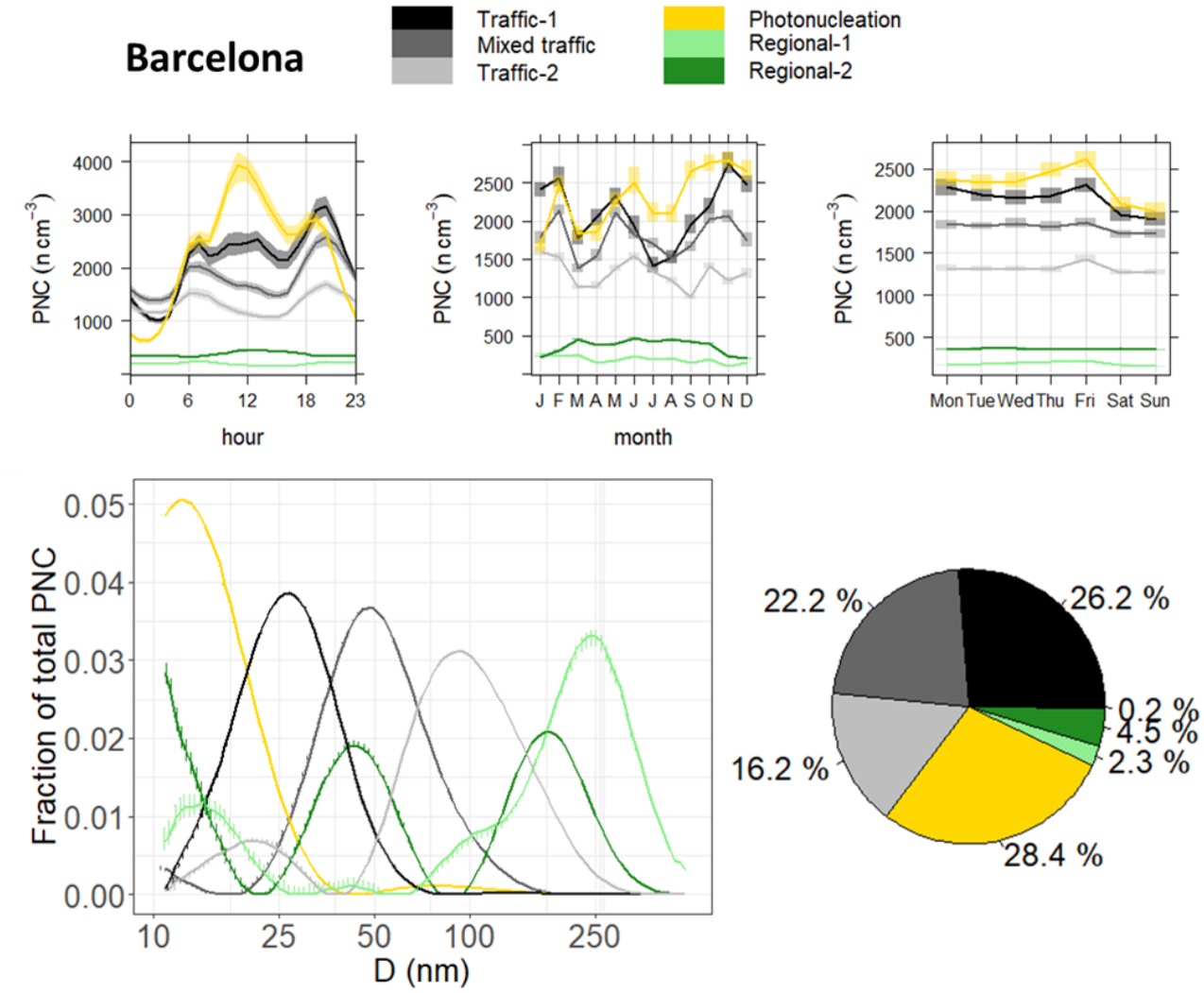

Figure 17. *Source apportionment results of Barcelona: daily, monthly and weekly patterns of the sources (top), particle number size distribution profiles (bottom left) and relative contributions (%) of particle number concentration (bottom right).*

In Athens, *Traffic-1* and *Mixed traffic* displayed similar profiles and patterns to those observed in Barcelona, with peaks during traffic rush hours and lower values during summer and on weekends. *Traffic-1*, with a primary size mode at 25-30 nm, contributed 21% to the total PNC and is associated with gasoline emissions and the nucleation of particles generated during the dilution of diesel exhaust SVOCs. *Mixed traffic* accounted for 25% of the total PNC. At this site, *Traffic-2* was not identified as a separate source but was combined with significant contributions from

RI-URBANS (www.RIURBANS.eu) is supported by the European Commission under the Horizon 2020 – Research and Innovation Framework Programme, H2020-GD-2020, Grant Agreement number: 101036245

Domestic heating. This *Traffic-2 + Domestic heating* source contributed 29% to the total PNC and is characterized by a primary size mode at 80 nm. It exhibited high PNC concentrations during traffic rush hours, as well as elevated levels at night, on weekends, and particularly during winter, when domestic burning is more frequent (Kleeman et al., 2009; Gu et al., 2011; Corsini et al., 2019). This source also showed high contributions to the variance of BC. *Photonucleation*, with a primary size mode at 17 nm, contributed 28% to the total PNC and exhibited a pronounced peak at midday. *Urban background*, characterised by a primary size mode at 160 nm, contributed 9% to the total PNC. This source can be described as a heavily traffic-influenced urban background, following similar traffic profiles and patterns but with a coarser mode, representing aged traffic particles that had grown after their initial emission. *Regional background*, in the accumulation mode, accounted for 4% of the total PNC and represents a mix of the two regional sources described before.

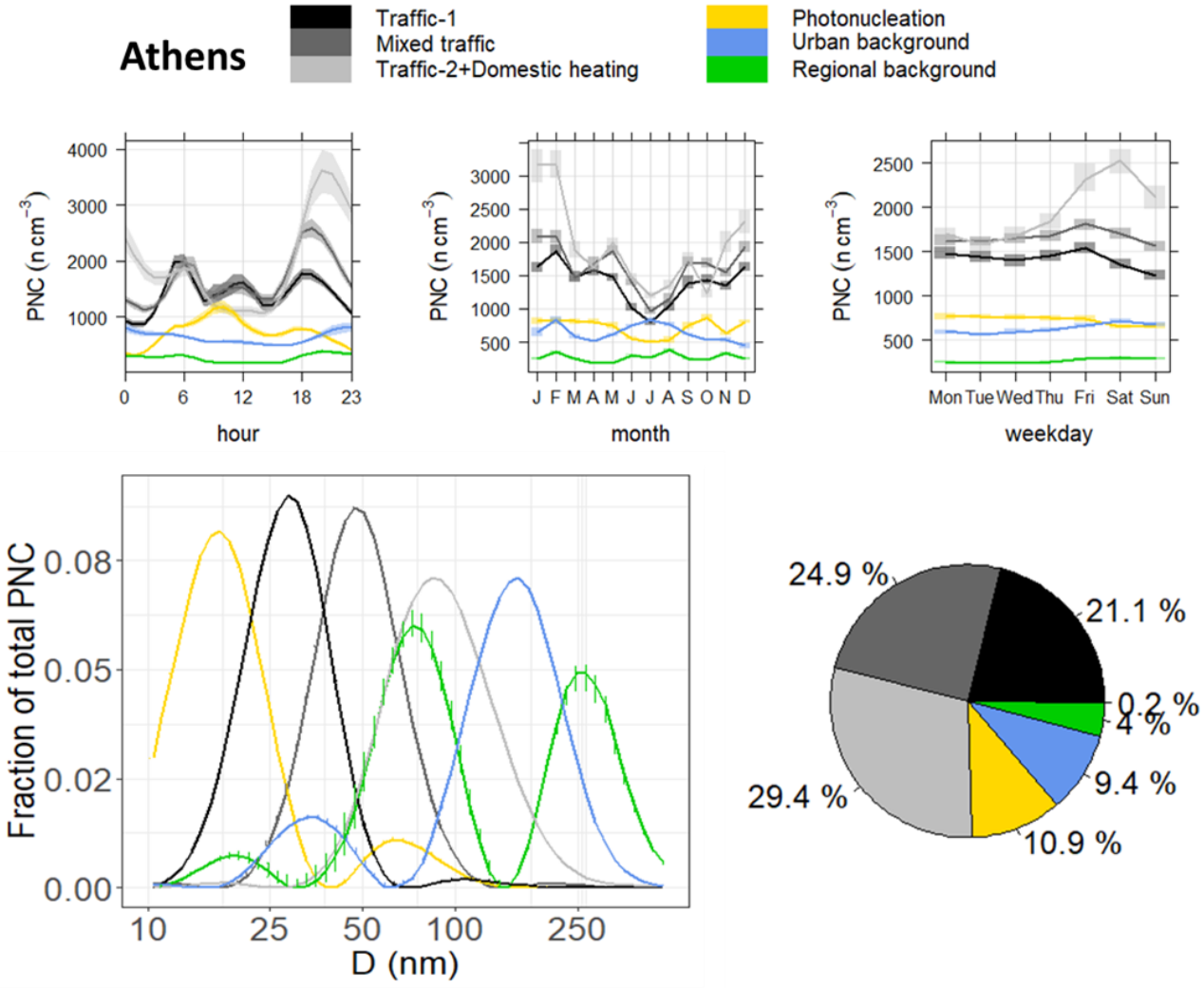

Figure 18. *Source apportionment results of Athens: daily, monthly and weekly patterns of the sources (top), particle number size distribution profiles (bottom left) and relative contributions (%) of particle number concentration (bottom right).*

RI-URBANS (www.RIURBANS.eu) is supported by the European Commission under the Horizon 2020 – Research and Innovation Framework Programme, H2020-GD-2020, Grant Agreement number: 101036245

In Paris, *Traffic-1* and *Mixed traffic* displayed profiles and patterns similar to those observed in Barcelona and Athens. *Traffic-1*, with a primary size mode at 22 nm, contributed 30% to the total PNC, while *Mixed traffic*, with a primary size mode at 46 nm, accounted for 23% of the total PNC. *Domestic heating*, characterised by a primary size mode at 102 nm, contributed 12% to the total PNC. This source exhibited higher levels at night and significant contributions to the variance of BC. It may also include particles from *Traffic-2*, albeit to a lesser extent, due to the absence of pronounced traffic rush hour patterns. *Nucleation*, with a primary size mode at 13 nm, accounted for 23% of the total PNC. This source represents a mix of *Photonucleation* and the nucleation of particles immediately after the emission of SVOCs from diesel vehicles. as these compounds dilute and cool in the atmosphere, leading to NPF (Harrison et al., 2011; Mamakos and Martini, 2011; Trechera et al., 2023; Saarikoski et al., 2024), due to the marked traffic rush hour patterns. As in Barcelona, two regional sources were identified at this site, both with peaks in the accumulation mode. *Regional-1*, contributing 2% of the total PNC, is associated with nitrates formed during winter and at night. *Regional-2*, accounting for 11% of the PNC, is linked to secondary ammonium sulphate and organic aerosols, with high contributions to the variance of ozone.

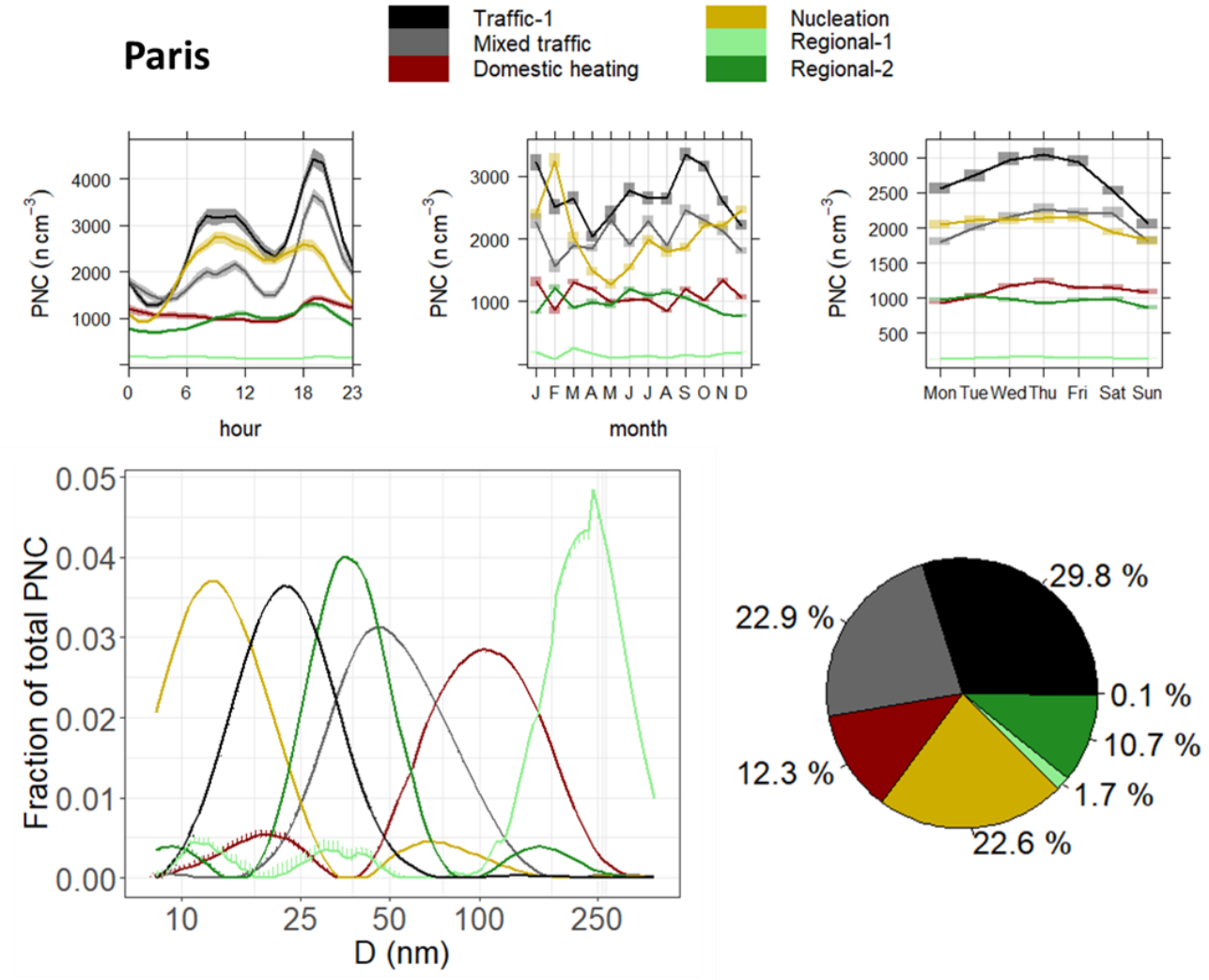

Figure 19. *Source apportionment results of Paris: daily, monthly and weekly patterns of the sources (top), particle number size distribution profiles (bottom left) and relative contributions (%) of particle number concentration (bottom right).*

RI-URBANS (www.RIURBANS.eu) is supported by the European Commission under the Horizon 2020 – Research and Innovation Framework Programme, H2020-GD-2020, Grant Agreement number: 101036245

The source apportionment results for Barcelona and Athens from this study (2020-2023) are consistent with those reported by Garcia-Marlès et al. (2024b) for the period 2009-2019.

4 Summary and Recommendations

The presented work leveraged Service Tools (STs) developed within other work packages of RI-URBANS to achieve significant progress in characterization of particulate matter (PM) and source apportionment (SA), including equivalent black carbon (eBC) and particle number size distribution (PNSD). Tools designed for online and offline chemical speciation (e.g., ST2, ST3) were successfully applied to generate input datasets for source apportionment purposes (e.g., ST10, ST11), providing valuable insights into the contributions of various PM sources. Additionally, the use of non-targeted mass spectral analyses showed promise in further identifying the organic composition of PM, particularly for advancing the understanding of organic aerosol (OA) sources. STs for oxidative potential (OP) measurement (e.g., ST4) and source apportionment (e.g., ST11) were also successfully implemented, demonstrating their ability to link temporal variations in PM sources to OP and to target specific local sources for each pilot city. These tools highlighted the potential for more robust assessments of health-relevant PM characteristics. Similarly, STs for ultrafine particle (UFP)-PNSD measurement and source apportionment (e.g., ST1 and ST11, respectively) proved effective in improving understanding of UFP sources. We recommend following the STs used within this document. Implementing the full scale of UFP characterization and aerosol chemistry measurements of the new air quality directive with a harmonized approach described in RI-URBANS STs will provide critical new information on the connection between air quality and health impacts.

A key accomplishment of this whole work package (WP4) was the generation of yearlong datasets of PM constituents and types. These datasets are invaluable for epidemiological studies, enabling assessments of the harmfulness of specific PM components and their broader implications for human health. This contribution provides a robust foundation for evaluating PM impacts and informing targeted air quality management strategies. Such datasets are also of utmost importance for modelling purposes and cross-validation for CTM results.

Despite the advancements achieved, further research is required to address several critical challenges. A major area for improvement lies in differentiating closely related PM sources, such as exhaust versus non-exhaust traffic emissions and primary versus secondary biomass burning particles. These distinctions are vital for refining OP source apportionment and interpreting PM characteristics more accurately. There is also a need to improve understanding of the origins and formation processes of nitrate-rich and sulfate-rich PM, which are currently broadly categorized as secondary PM (including also e.g., secondary organic aerosols, SOA, of unclear origin). The environmental significance and origins of these PM types remain unclear, limiting their interpretation. Similarly, some organic carbon (OC) types identified through non-targeted analyses lack sufficient environmental context, posing challenges for attributing OP contributions to specific PM sources. It is also recommended for the SIA and SOA to couple receptor modelling with chemical transport models. For example, to elucidate the origin of ammonium sulphate and nitrate sources from the receptor modelling.

Another key area requiring attention is the optimal use of size-segregated PM information. While size-resolved data offer significant potential for source attribution and health effect assessments, current methodologies do not fully leverage this dimension. Future research should focus on integrating size-segregated data into source apportionment frameworks to maximize its utility. Finally, the reliance on temporal variations in existing methodologies, such as multilinear regression, highlights the need for new approaches that incorporate spatial and size-segregated data. Addressing this limitation could enhance the robustness and sensitivity of OP source apportionment results, making them more applicable to a wider range of air quality and health studies.

RI-URBANS (www.RIURBANS.eu) is supported by the European Commission under the Horizon 2020 – Research and Innovation Framework Programme, H2020-GD-2020, Grant Agreement number: 101036245

Overall, this deliverable underscores the effective application of STs to address key challenges in PM characterization and source apportionment. The outcomes demonstrate significant progress in understanding PM sources, equivalent black carbon (eBC), and UFP-PNSD as well as their potential health-relevance based on their OP while also identifying areas for future research. Further efforts to refine source distinctions, interpret complex PM compositions, and utilize size-segregated information will be essential for advancing PM health impact assessments and guiding targeted mitigation strategies.

To improve the understanding of M)sources, combining chemical speciation with statistical receptor models has proven to be a powerful approach. However, this method requires the measurement of a wide range of chemical constituents over a minimum duration of one year, which can entail substantial costs. To optimize source apportionment of PM10, it is recommended to include measurements of key components such as elemental carbon (EC), organic carbon (OC), as well as organic marker compounds arabitol and/or mannitol, levoglucosan, 3-MBTCA, 2-methlythreitol, methanesulfonic acid (MSA), and water-soluble inorganic constituents such as chloride (Cl-), nitrate (NO3-), sulfate (SO42-), ammonium (NH4+), and total element concentrations of sodium (Na), magnesium (Mg), potassium (K), calcium (Ca), iron (Fe), titanium (Ti), vanadium (V), copper (Cu), rubidium (Rb), tin (Sn), lead (Pb), aluminum (Al), manganese (Mn), nickel (Ni), and zinc (Zn), chromium (Cr), cadmium (Cd), arsenic (As), barium (Ba), antimony (Sb), selenium (Se), and other emerging tracers. Additionally, for oxidative potential (OP) source apportionment, which currently relies on temporal variations of PM sources, we recommend compiling datasets spanning at least one year, with samples collected at the very least every fourth day for 24 hours (preferably 3rd day), though for epidemiological assessments a higher frequency might be needed. This temporal resolution is critical for robust analyses. For UFPs, similar long-term datasets should be compiled, ensuring consistency and comparability across studies to enhance our understanding of these particle sources and their health impacts.

5 References

ACTRIS: Preliminary ACTRIS recommendation for aerosol in-situ sampling, measurements, and analysis. https://www.actris.eu/sites/default/files/2021-06/Preliminary%20ACTRIS%20recommendations%20for%20aerosol%20in-situ%20measurements%20June%202021.pdf, 2021.

Alastuey, A., Querol, X., Aas, W., Lucarelli, F., Pérez, N., Moreno, T., Cavalli, F., Areskoug, H., Balan, V., Catrambone, M., Ceburnis, D., Cerro, J. C., Conil, S., Gevorgyan, L., Hueglin, C., Imre, K., Jaffrezo, J. L., Leeson, S. R., Mihalopoulos, N., Mitosinkova, M., O'Dowd, C. D., Pey, J., Putaud, J. P., Riffault, V., Ripoll, A., Sciare, J., Sellegri, K., Spindler, G., and Yttri, K. E.: Geochemistry of PM10 over Europe during the EMEP intensive measurement periods in summer 2012 and winter 2013, Atmos. Chem. Phys., 16, 6107-6129, 10.5194/acp-16-6107-2016, 2016.

Alier, M., van Drooge, B. L., Dall'Osto, M., Querol, X., Grimalt, J. O., and Tauler, R.: Source apportionment of submicron organic aerosol at an urban background and a road site in Barcelona (Spain) during SAPUSS, Atmos. Chem. Phys., 13, 10353-10371, 10.5194/acp-13-10353-2013, 2013.

Amato, F., Pandolfi, M., Escrig, A., Querol, X., Alastuey, A., Pey, J., Perez, N., and Hopke, P. K.: Quantifying road dust resuspension in urban environment by Multilinear Engine: A comparison with PMF2, Atmospheric Environment, 43, 2770-2780, https://doi.org/10.1016/j.atmosenv.2009.02.039, 2009.

RI-URBANS (www.RIURBANS.eu) is supported by the European Commission under the Horizon 2020 – Research and Innovation Framework Programme, H2020-GD-2020, Grant Agreement number: 101036245

Atwi, K., Cheng, Z., El Hajj, O., Perrie, C., and Saleh, R.: A dominant contribution to light absorption by methanol-insoluble brown carbon produced in the combustion of biomass fuels typically consumed in wildland fires in the United States, Environmental Science: Atmospheres, 2, 182-191, 10.1039/D1EA00065A, 2022.

Belis, C. A., Favez, O., Mircea, M., Diapouli, E., Manousakas, M. I., Vratolis, S., Gilardoni, S., Paglione, M., Decesari, S., Mocnik, G., Mooibroek, D., Salvador, P., Takahama, S., Vecchi, R., and Paatero, P.: European guide on air pollution source apportionment with receptor models - Revised version 2019. EUR 29816 EN. , Joint Research Centre (European Commission). JRC117306. Publications Office of the European Union, Luxembourg, 2019. https://data.europa.eu/doi/10.2760/439106, 2019.

Borlaza, L. J. S., Weber, S., Uzu, G., Jacob, V., Cañete, T., Micallef, S., Trébuchon, C., Slama, R., Favez, O., and Jaffrezo, J. L.: Disparities in particulate matter (PM10) origins and oxidative potential at a city scale (Grenoble, France) – Part 1: Source apportionment at three neighbouring sites, Atmos. Chem. Phys., 21, 5415-5437, 10.5194/acp-21-5415-2021, 2021.

Brines, M., Dall'Osto, M., Beddows, D.C.S., Harrison, R.M., Gomez-Moreno, F., Núnez, L., Artínano, B., Costabile, F., Gobbi, G.P., Salimi, F., Morawska, L., Sioutas, C. and Querol, X.: Traffic and nucleation events as main sources of ultrafine particles in high-insolation developed world cities, Atmos. Chem. Phys. 15, 5929–5945, https://doi.org/10.5194/acp-15-5929-2015, 2015.

Brown, R. J., Beccaceci, S., Butterfield, D. M., Quincey, P. G., Harris, P. M., Maggos, T., Panteliadis, P., John, A., Jedynska, A., and Kuhlbusch, T. A.: Standardisation of a European measurement method for organic carbon and elemental carbon in ambient air: results of the field trial campaign and the determination of a measurement uncertainty and working range, Environmental Science: Processes & Impacts, 19, 1249-1259, 2017.

Calas, A., Uzu, G., Martins, J. M. F., Voisin, D., Spadini, L., Lacroix, T., and Jaffrezo, J.-L.: The importance of simulated lung fluid (SLF) extractions for a more relevant evaluation of the oxidative potential of particulate matter, Scientific Reports, 7, 11617, 10.1038/s41598-017-11979-3, 2017.

Calas, A., Uzu, G., Kelly, F. J., Houdier, S., Martins, J. M., Thomas, F., Molton, F., Charron, A., Dunster, C., and Oliete, A.: Comparison between five acellular oxidative potential measurement assays performed with detailed chemistry on PM 10 samples from the city of Chamonix (France), Atmos. Chem. Phys., 18, 7863-7875, 2018.

Calas, A., Uzu, G., Besombes, J.-L., Martins, J. M. F., Redaelli, M., Weber, S., Charron, A., Albinet, A., Chevrier, F., Brulfert, G., Mesbah, B., Favez, O., and Jaffrezo, J.-L.: Seasonal Variations and Chemical Predictors of Oxidative Potential (OP) of Particulate Matter (PM), for Seven Urban French Sites, Atmosphere, 10, 698, 2019.

Carslaw, D. C. and Ropkins, K.: openair — An R package for air quality data analysis, Environmental Modelling & Software, 27-28, 52-61, https://doi.org/10.1016/j.envsoft.2011.09.008, 2012.

Cavalli, F., Viana, M., Yttri, K. E., Genberg, J., and Putaud, J. P.: Toward a standardised thermal-optical protocol for measuring atmospheric organic and elemental carbon: the EUSAAR protocol, Atmos. Meas. Tech., 3, 79-89, 10.5194/amt-3-79-2010, 2010.

CEN/–S16976:2016: CEN Standard for Ambient air - Determination of the particle number concentration of atmospheric aerosol. https://standards.iteh.ai/catalog/standards/cen/91f1ac67-f6d6-408c-af89-e81763194fd3/cen-ts-16976-2016.

CEN/TS17434:2020: Standard for Ambient air - Determination of the particle number size distribution of atmospheric aerosol using a Mobility Particle Size Spectrometer (MPSS). https://standards.iteh.ai/catalog/standards/cen/a841bc08-ed34-4fa8-94ca-8c5e07b99db9/cen-ts-17434-2020.

RI-URBANS (www.RIURBANS.eu) is supported by the European Commission under the Horizon 2020 – Research and Innovation Framework Programme, H2020-GD-2020, Grant Agreement number: 101036245

Corsini, E., Marinovich, M., Vecchi, R.: Ultrafine particles from residential biomass combustion: a review on experimental data and toxicological response, Int. J. Mol. Sci. 20 (20), 4992, https://doi.org/10.3390/ijms20204992, 2019.

Cui, T., Manousakas, M. I., Wang, Q., Uzu, G., Hao, Y., Khare, P., Qi, L., Chen, Y., Han, Y., Slowik, J. G., Jaffrezo, J.-L., Cao, J., Prévôt, A. S. H., and Daellenbach, K. R.: Composition and Sources of Organic Aerosol in Two Megacities in Western China Using Complementary Mass Spectrometric and Statistical Techniques, ACS ES&T Air, 10.1021/acsestair.4c00051, 2024.

Daellenbach, K. R., Uzu, G., Jiang, J., Cassagnes, L.-E., Leni, Z., Vlachou, A., Stefenelli, G., Canonaco, F., Weber, S., and Segers, A.: Sources of particulate-matter air pollution and its oxidative potential in Europe, Nature, 587, 414-419, https://doi.org/10.1038/s41586-020-2902-8, 2020.

Daellenbach, K. R., Bozzetti, C., Křepelová, A., Canonaco, F., Wolf, R., Zotter, P., Fermo, P., Crippa, M., Slowik, J. G., Sosedova, Y., Zhang, Y., Huang, R. J., Poulain, L., Szidat, S., Baltensperger, U., El Haddad, I., and Prévôt, A. S. H.: Characterization and source apportionment of organic aerosol using offline aerosol mass spectrometry, Atmos. Meas. Tech., 9, 23-39, https://doi.org/10.5194/amt-9-23-2016, 2016.

Dall'Osto, M., Harrison, R.M., Coe, H., Williams, P.I., Allan, J.D.: Real time chemical characterization of local and regional nitrate aerosols, Atmos. Chem. Phys. 9, 3709–3720, https://doi.org/10.5194/acp-9-3709-2009, 2009.

Damayanti, S., Harrison, R.M., Pope, F., Beddows, D.C.S.: Limited impact of diesel particle filters on road traffic emissions of ultrafine particles, Environ. Int. 174, 107888, https://doi.org/10.1016/j.envint.2023.107888, 2023.

Drinovec, L., Močnik, G., Zotter, P., Prévôt, A. S. H., Ruckstuhl, C., Coz, E., Rupakheti, M., Sciare, J., Müller, T., Wiedensohler, A., and Hansen, A. D. A.: The "dual-spot" Aethalometer: an improved measurement of aerosol black carbon with real-time loading compensation, Atmos. Meas. Tech., 8, 1965-1979, 10.5194/amt-8-1965-2015, 2015.

Ehn, M., Thornton, J., Kleist, E., Sipila, M., Junninen, H., Pullinen, I., Springer, M., Rubach, F., Tillmann, R., Lee, B., Lopez-Hilfiker, F., Andres, S., Acir, I.H., Rissanen, M., Jokinen, T., Schobesberger, S., Kangasluoma, J., Kontkanen, J., Nieminen, T., Kurtén, T., Nielsen, L.B., Jørgensen, S., Kjaergaard, H.G., Canagaratna, M., Dal Maso, M., Berndt, T., Petäjä, T., Wahner, A., Kerminen, V.M., Kulmala, M., Worsnop, D.R., Wildt, J., Mentel, T.F.: A large source of low volatility secondary organic aerosol, Nature 506, 476–479, https://doi.org/ 10.1038/nature13032, 2014.

EN12341:2023 'Ambient Air — Standard gravimetric measurement method for the determination of the PM10 or PM2.5 mass concentration of suspended particulate matter', CEN, Brussels.

EN16450:2017 'Ambient air - Automated measuring systems for the measurement of the concentration of particulate matter (PM10; PM2,5)', CEN, Brussels

EN16909:2017: European Committee for Standardisation (CEN). Ambient Air Measurement of Elemental Carbon (EC) and Organic Carbon (OC) Collected on Filters.

EN16913:2017: 'Ambient air - Standard method for measurement of NO3-, SO42-, Cl-, NH4+, Na+, K+, Mg2+, Ca2+ in PM2.5 as deposited on filters'.

EU, 2008. Directive 2008/50/EC of the European Parliament and of the Council of 21 May 2008 on ambient air quality and cleaner air for Europe, Off. J. EU; https://eur-lex.europa.eu/eli/dir/2008/50/oj.

EU, 2024. Directive of the European Parliament and of the Council of 23 October 2024 on ambient air quality and cleaner air for Europe (recast). https://eur-lex.europa.eu/eli/dir/2024/2881/oj

RI-URBANS (www.RIURBANS.eu) is supported by the European Commission under the Horizon 2020 – Research and Innovation Framework Programme, H2020-GD-2020, Grant Agreement number: 101036245

Fontal, M., van Drooge, B. L., López, J. F., Fernández, P., and Grimalt, J. O.: Broad spectrum analysis of polar and apolar organic compounds in submicron atmospheric particles, Journal of Chromatography A, 1404, 28-38, https://doi.org/10.1016/j.chroma.2015.05.042, 2015.

Garcia-Marlès, M., Lara, R., Reche, C., Pérez, N., Tobías, A., Savadkoohi, M., Beddows, D., Salma, I., Vörösmarty, M., Weidinger, T., Hueglin, C., Mihalopoulos, N., Grivas, G., Kalkavouras, P., Ondráček, J., Zíková, N., Niemi, J. V., Manninen, H. E., Green, D. C., Tremper, A. H., Norman, M., Vratolis, S., Eleftheriadis, K., Gómez-Moreno, F. J., Alonso-Blanco, E., Wiedensohler, A., Weinhold, K., Merkel, M., Bastian, S., Hoffmann, B., Altug, H., Petit, J.-E., Favez, O., Dos Santos, S. M., Putaud, J.-P., Dinoi, A., Contini, D., Timonen, H., Lampilahti, J., Petäjä, T., Pandolfi, M., Hopke, P. K., Harrison, R. M., Alastuey, A., and Querol, X.: Inter-annual trends of ultrafine particles in urban Europe, Environment International, 185, 108510, https://doi.org/10.1016/j.envint.2024.108510, 2024a.

Garcia-Marlès, M., Lara, R., Reche, C., Pérez, N, Tobías, A., Savadkoohi, M., Beddows, D., Salma, I., Vörösmarty, M., Weidinger, T., Hueglin, C., Mihalopoulos, N., Grivas, G., Kalkavouras, P., Ondráček, J., Zíková, N., Niemi, J.V., Manninen, H.E., Green, D.C., Tremper, A.H., Norman, M., Vratolis, S., Diapouli, E., Eleftheriadis, K., Gómez-Moreno, F.J., Alonso-Blanco, E., Wiedensohler, A., Weinhold, K., Merkel, M., Bastian, S., Hoffmann, B., Altug, H., Petit, J.E., Acharja, P., Favez, O., Dos Santos, S.M., Putaud, J.P., Dinoi, A., Contini, D., Casans, A., Casquero-Vera, J.A., Crumeyrolle, S., Bourrianne, E., Van Poppel, M., Dreesen, F.E., Harni, S., Timonen, H., Lampilahti, J., Petäjä, T., Pandolfi, M., Hopke, P.K., Harrison, R.M., Alastuey, A., and Querol, X.: Source apportionment of ultrafine particles in urban Europe. Environment International, 194, 109149, https://doi.org/10.1016/j.envint.2024.109149, 2024b.

Gianini, M. F. D., Piot, C., Herich, H., Besombes, J. L., Jaffrezo, J. L., and Hueglin, C.: Source apportionment of PM10, organic carbon and elemental carbon at Swiss sites: An intercomparison of different approaches, Science of The Total Environment, 454-455, 99-108, https://doi.org/10.1016/j.scitotenv.2013.02.043, 2013.

Glojek, K., Dinh Ngoc Thuy, V., Weber, S., Uzu, G., Manousakas, M., Elazzouzi, R., Džepina, K., Darfeuil, S., Ginot, P., Jaffrezo, J. L., Žabkar, R., Turšič, J., Podkoritnik, A., and Močnik, G.: Annual variation of source contributions to PM10 and oxidative potential in a mountainous area with traffic, biomass burning, cement-plant and biogenic influences, Environment International, 189, 108787, https://doi.org/10.1016/j.envint.2024.108787, 2024.

Gu, J., Pitz, M., Schnelle-Kreis, J., Diemer, J., Reller, A., Zimmermann, R., Soentgen, J., Stoelzel, M., Wichmann, H.E., Peters, A., Cyrys, J.: Source apportionment of ambient particles: comparison of positive matrix factorization analysis applied to particle size distribution and chemical composition data, Atmos. Environ. 45 (10), 1849–1857, https://doi.org/10.1016/j.atmosenv.2011.01.009, 2011.

Harrison, R.M., Beddows, D.C.S., Dall'Osto, M.: PMF analysis of wide-range particle size spectra collected on a major highway, Environ. Sci. Technol. 45, 5522–5528, https://doi.org/10.1021/es2006622, 2011.

Hecobian, A., Zhang, X., Zheng, M., Frank, N., Edgerton, E. S., and Weber, R. J.: Water-Soluble Organic Aerosol material and the light-absorption characteristics of aqueous extracts measured over the Southeastern United States, Atmos. Chem. Phys., 10, 5965-5977, 10.5194/acp-10-5965-2010, 2010.

Hopke, P.K., Feng, Y., Dai, Q.: Source apportionment of particle number concentrations: a global review, Sci. Total Environ. 819, 153104, https://doi.org/ 10.1016/j.scitotenv.2022.153104, 2022.

Hopke, P. K., Chen, Y., Rich, D. Q., Mooibroek, D., and Sofowote, U. M.: The application of positive matrix factorization with diagnostics to BIG DATA, Chemometrics and Intelligent Laboratory Systems, 240, 104885, https://doi.org/10.1016/j.chemolab.2023.104885, 2023.

RI-URBANS (www.RIURBANS.eu) is supported by the European Commission under the Horizon 2020 – Research and Innovation Framework Programme, H2020-GD-2020, Grant Agreement number: 101036245

Hopke, P.K., Chen, Y., Chalupa, D.C., Rich, D.Q.: Long term trends in source apportioned particle number concentrations in Rochester NY, Environ. Pollut. 347, 123708. https://doi.org/10.1016/j.envpol.2024.123708, 2024.

Karanasiou, A., Minguillón, M. C., Viana, M., Alastuey, A., Putaud, J. P., Maenhaut, W., Panteliadis, P., Močnik, G., Favez, O., and Kuhlbusch, T. A. J.: Thermal-optical analysis for the measurement of elemental carbon (EC) and organic carbon (OC) in ambient air a literature review, Atmos. Meas. Tech. Discuss., 2015, 9649-9712, 10.5194/amtd-8-9649-2015, 2015.

Kleeman, M.J., Riddle, S.G., Robert, M.A., Jakober, C.A., Fine, P.M., Hays, M.D., Schauer, J.J., Hannigan, M.P.: Source apportionment of fine (PM1.8) and ultrafine (PM0.1) airborne particulate matter during a severe winter pollution episode, Environ. Sci. Technol. 43, 2, 272–279, https://doi.org/10.1021/ es800400m, 2009.

Kulmala, M., Kerminen, V.M.: On the formation and growth of atmospheric nanoparticles, Atmos. Res. 90 (2–4), 132–150, https://doi.org/10.1016/j. atmosres.2008.01.005, 2008.

Liu, Z.R., Hu, B., Liu, Q., Sun, Y., Wang, Y.S.: Source apportionment of urban fine particle number concentration during summertime in Beijing, Atmos. Environ. 96, 359–369, https://doi.org/10.1016/j.atmosenv.2014.06.055, 2014.

Mamakos, A., Martini, G.: Particle Number Emissions During Regeneration of DPFequipped Light Duty Diesel Vehicles - a Literature Survey. EUR 24853 EN. Publications Office of the European Union, Luxembourg. JRC64870, 2011.

Masiol, M., Vu, T.V., Beddows, D.C.S., Harrison, R.M.: Source apportionment of wide range particle size spectra and black carbon collected at the airport of Venice (Italy), Atmos. Environ. 139, 56–74, https://doi.org/10.1016/j. atmosenv.2016.05.018, 2016.

Mircea, M., Calori, G., Pirovano, G., and Belis, C.: European guide on air pollution source apportionment for particulate matter with source-oriented models and their combined use with receptor models. , EUR 30082 EN, Publications Office of the European Union, Luxembourg. , 10.2760/470628, JRC119067, 2020.

Moreno, T., Querol, X., Alastuey, A., Viana, M., Salvador, P., Sánchez de la Campa, A., Artiñano, B., de la Rosa, J., and Gibbons, W.: Variations in atmospheric PM trace metal content in Spanish towns: Illustrating the chemical complexity of the inorganic urban aerosol cocktail, Atmospheric Environment, 40, 6791-6803, https://doi.org/10.1016/j.atmosenv.2006.05.074, 2006.

Norris, G., Duvall, R., Brown, S., and Bai, S.: EPA Positive Matrix Factorization (PMF) 5.0 Fundamentals and User Guide, 2014.

Nozaki, Y.: A fresh look at element distribution in the North Pacific Ocean, Eos, Transactions American Geophysical Union, 78, 221-221, https://doi.org/10.1029/97EO00148, 1997.

Ogulei, D., Hopke, P.K., Chalupa, D.C., Utell, M.J.: Modeling source contributions to submicron particle number concentrations measured in rochester. New York, Aerosol Sci. Technol. 41, 179–201, https://doi.org/10.1080/02786820601116012, 2007.

Paatero, P.: The multilinear engine—a table-driven, least squares program for solving multilinear problems, including the n-way parallel factor analysis model, J. Comput. Graph. Stat. 8, 854-888, https://doi.org/10.1080/10618600.1999.10474853, 1999.

Paatero, P. and Tapper, U.: Positive matrix factorization: A non-negative factor model with optimal utilization of error estimates of data values, Environmentrics, 5, 111-126, https://doi.org/10.1002/env.3170050203, 1994.

RI-URBANS (www.RIURBANS.eu) is supported by the European Commission under the Horizon 2020 – Research and Innovation Framework Programme, H2020-GD-2020, Grant Agreement number: 101036245

Paraskevopoulou, D., Liakakou, E., Gerasopoulos, E., and Mihalopoulos, N.: Sources of atmospheric aerosol from long-term measurements (5years) of chemical composition in Athens, Greece, Science of The Total Environment, 527-528, 165-178, https://doi.org/10.1016/j.scitotenv.2015.04.022, 2015.

Paraskevopoulou, D., Kaskaoutis, D. G., Grivas, G., Bikkina, S., Tsagkaraki, M., Vrettou, I. M., Tavernaraki, K., Papoutsidaki, K., Stavroulas, I., Liakakou, E., Bougiatioti, A., Oikonomou, K., Gerasopoulos, E., and Mihalopoulos, N.: Brown carbon absorption and radiative effects under intense residential wood burning conditions in Southeastern Europe: New insights into the abundance and absorptivity of methanol-soluble organic aerosols, Science of The Total Environment, 860, 160434, https://doi.org/10.1016/j.scitotenv.2022.160434, 2023.

Querol, X., Alastuey, A., Rodriguez, S., Plana, F., Ruiz, C. R., Cots, N., Massagué, G., and Puig, O.: PM10 and PM2.5 source apportionment in the Barcelona Metropolitan area, Catalonia, Spain, Atmospheric Environment, 35, 6407-6419, https://doi.org/10.1016/S1352-2310(01)00361-2, 2001.

Sandradewi, J., Prévôt, A. S. H., Szidat, S., Perron, N., Alfarra, M. R., Lanz, V. A., Weingartner, E., and Baltensperger, U.: Using Aerosol Light Absorption Measurements for the Quantitative Determination of Wood Burning and Traffic Emission Contributions to Particulate Matter, Environmental Science & Technology, 42, 3316-3323, 10.1021/es702253m, 2008.

Saarikoski, S., Järvinen, A., Markkula, L., Aurela, M., Kuittinen, N., Hoivala, J., Barreira, L.M.F., Aakko-Saksa, P., Lepisto, T., Marjanen, P., Timonen, H., Hakkarainen, H., Jalava, P., Ronkkö, T.: Towards zero pollution vehicles by advanced fuels and exhaust aftertreatment technologies, Environ. Pollut. 347, 123665, https://doi.org/10.1016/j.envpol.2024.123665, 2024.

Savadkoohi, M., Pandolfi, M., Reche, C., Niemi, J. V., Mooibroek, D., Titos, G., Green, D. C., Tremper, A. H., Hueglin, C., Liakakou, E., Mihalopoulos, N., Stavroulas, I., Artiñano, B., Coz, E., Alados-Arboledas, L., Beddows, D., Riffault, V., De Brito, J. F., Bastian, S., Baudic, A., Colombi, C., Costabile, F., Chazeau, B., Marchand, N., Gómez-Amo, J. L., Estellés, V., Matos, V., van der Gaag, E., Gille, G., Luoma, K., Manninen, H. E., Norman, M., Silvergren, S., Petit, J.-E., Putaud, J.-P., Rattigan, O. V., Timonen, H., Tuch, T., Merkel, M., Weinhold, K., Vratolis, S., Vasilescu, J., Favez, O., Harrison, R. M., Laj, P., Wiedensohler, A., Hopke, P. K., Petäjä, T., Alastuey, A., and Querol, X.: The variability of mass concentrations and source apportionment analysis of equivalent black carbon across urban Europe, Environment International, 178, 108081, https://doi.org/10.1016/j.envint.2023.108081, 2023.

Seinfeld, J.H., Pandis, S.: Atmospheric Chemistry and Physics: From Air Pollution to Climate Change, 3rd Edition. Wiley. ISBN 10: 1118947401, 2016.

Shetty, N. J., Pandey, A., Baker, S., Hao, W. M., and Chakrabarty, R. K.: Measuring light absorption by freshly emitted organic aerosols: optical artifacts in traditional solvent-extraction-based methods, Atmos. Chem. Phys., 19, 8817-8830, 10.5194/acp-19-8817-2019, 2019.

Srinivas, B., Rastogi, N., Sarin, M. M., Singh, A., and Singh, D.: Mass absorption efficiency of light absorbing organic aerosols from source region of paddy-residue burning emissions in the Indo-Gangetic Plain, Atmospheric Environment, 125, 360-370, https://doi.org/10.1016/j.atmosenv.2015.07.017, 2016.

Theodosi, C., Tsagkaraki, M., Zarmpas, P., Grivas, G., Liakakou, E., Paraskevopoulou, D., Lianou, M., Gerasopoulos, E., and Mihalopoulos, N.: Multi-year chemical composition of the fine-aerosol fraction in Athens, Greece, with emphasis on the contribution of residential heating in wintertime, Atmos. Chem. Phys., 18, 14371-14391, 10.5194/acp-18-14371-2018, 2018.

Tobler, A. K., Skiba, A., Canonaco, F., Močnik, G., Rai, P., Chen, G., Bartyzel, J., Zimnoch, M., Styszko, K., Nęcki, J., Furger, M., Różański, K., Baltensperger, U., Slowik, J. G., and Prevot, A. S. H.: Characterization of non-refractory

RI-URBANS (www.RIURBANS.eu) is supported by the European Commission under the Horizon 2020 – Research and Innovation Framework Programme, H2020-GD-2020, Grant Agreement number: 101036245

(NR) PM1 and source apportionment of organic aerosol in Kraków, Poland, Atmos. Chem. Phys., 21, 14893-14906, 10.5194/acp-21-14893-2021, 2021.

Trechera, P., Garcia-Marlès, M., Liu, X., Reche, C., Pérez, N., Savadkoohi, M., Beddows, D., Salma, I., Vörösmarty, M., Casans, A., Casquero-Vera, J. A., Hueglin, C., Marchand, N., Chazeau, B., Gille, G., Kalkavouras, P., Mihalopoulos, N., Ondracek, J., Zikova, N., Niemi, J. V., Manninen, H. E., Green, D. C., Tremper, A. H., Norman, M., Vratolis, S., Eleftheriadis, K., Gómez-Moreno, F. J., Alonso-Blanco, E., Gerwig, H., Wiedensohler, A., Weinhold, K., Merkel, M., Bastian, S., Petit, J.-E., Favez, O., Crumeyrolle, S., Ferlay, N., Martins Dos Santos, S., Putaud, J.-P., Timonen, H., Lampilahti, J., Asbach, C., Wolf, C., Kaminski, H., Altug, H., Hoffmann, B., Rich, D. Q., Pandolfi, M., Harrison, R. M., Hopke, P. K., Petäjä, T., Alastuey, A., and Querol, X.: Phenomenology of ultrafine particle concentrations and size distribution across urban Europe, Environment International, 172, 107744, https://doi.org/10.1016/j.envint.2023.107744, 2023.

van Drooge, B. L., Prats, R. M., Jaén, C., and Grimalt, J. O.: Determination of subpicogram levels of airborne polycyclic aromatic hydrocarbons for personal exposure monitoring assessment, Environmental Monitoring and Assessment, 195, 368, 10.1007/s10661-023-10953-z, 2023.

Vorösmarty, M., Hopke, P.K., Salma, I.: Attribution of aerosol particle number size distributions to main sources using an 11-year urban dataset, Atmos. Chem. Phys. 24, 5695–5712, https://doi.org/10.5194/acp-24-5695-2024, 2024.

Waked, A., Favez, O., Alleman, L., Piot, C., Petit, J.-E., Delaunay, T., Verlinden, E., Golly, B., Besombes, J.-L., and Jaffrezo, J.-L.: Source apportionment of PM10 in a north-western Europe regional urban background site (Lens, France) using positive matrix factorization and including primary biogenic emissions, Atmos. Chem. Phys., 14, 3325-3346, 2014.

Weber, S., Salameh, D., Albinet, A., Alleman, L. Y., Waked, A., Besombes, J.-L., Jacob, V., Guillaud, G., Meshbah, B., Rocq, B., Hulin, A., Dominik-Sègue, M., Chrétien, E., Jaffrezo, J.-L., and Favez, O.: Comparison of PM10 Sources Profiles at 15 French Sites Using a Harmonized Constrained Positive Matrix Factorization Approach, Atmosphere, 10, 310, 2019.

Weber S, Uzu G, Favez O, Borlaza L, Calas A, Salameh D, Chevrier F, Allard J, Besombes JL, Albinet A, Pontet S, Meshbah B, Gille G, Zhang S, Pallares C, Leoz-Garziandia E, and Jaffrezo JL (2021) Source apportionment of Oxidative Potential of atmospheric PM10: synthesis of 15 yearly time series in urban areas in France. Atmos. Chem. Phys., 10.5194/acp-2021-77

Zotter, P., Herich, H., Gysel, M., El-Haddad, I., Zhang, Y., Močnik, G., Hüglin, C., Baltensperger, U., Szidat, S., and Prévôt, A. S. H.: Evaluation of the absorption Ångström exponents for traffic and wood burning in the Aethalometer-based source apportionment using radiocarbon measurements of ambient aerosol, Atmos. Chem. Phys., 17, 4229-4249, 10.5194/acp-17-4229-2017, 2017.

RI-URBANS (www.RIURBANS.eu) is supported by the European Commission under the Horizon 2020 – Research and Innovation Framework Programme, H2020-GD-2020, Grant Agreement number: 101036245